

Y 3. At7

22/ CEX-58.9

AEC

RESEARCH REPORTS

AEC Category: PHYSICS

UNIVERSITY OF  
ARIZONA LIBRARY  
Documents Collection  
AUG 14 1961

# CEX-58.9

CIVIL EFFECTS STUDY

A MODEL DESIGNED TO PREDICT THE  
MOTION OF OBJECTS TRANSLATED  
BY CLASSICAL BLAST WAVES

I. Gerald Bowen, Ray W. Albright,  
E. Royce Fletcher, and Clayton S. White

Issuance Date: June 29, 1961

CIVIL EFFECTS TEST OPERATIONS  
U.S. ATOMIC ENERGY COMMISSION

## NOTICE

This report is published in the interest of providing information which may prove of value to the reader in his study of effects data derived principally from nuclear weapons tests.

This document is based on information available at the time of preparation which may have subsequently been expanded and re-evaluated. Also, in preparing this report for publication, some classified material may have been removed. Users are cautioned to avoid interpretations and conclusions based on unknown or incomplete data.

PRINTED IN USA

Price \$1.25. Available from the Office of  
Technical Services, Department of Commerce,  
Washington 25, D. C.

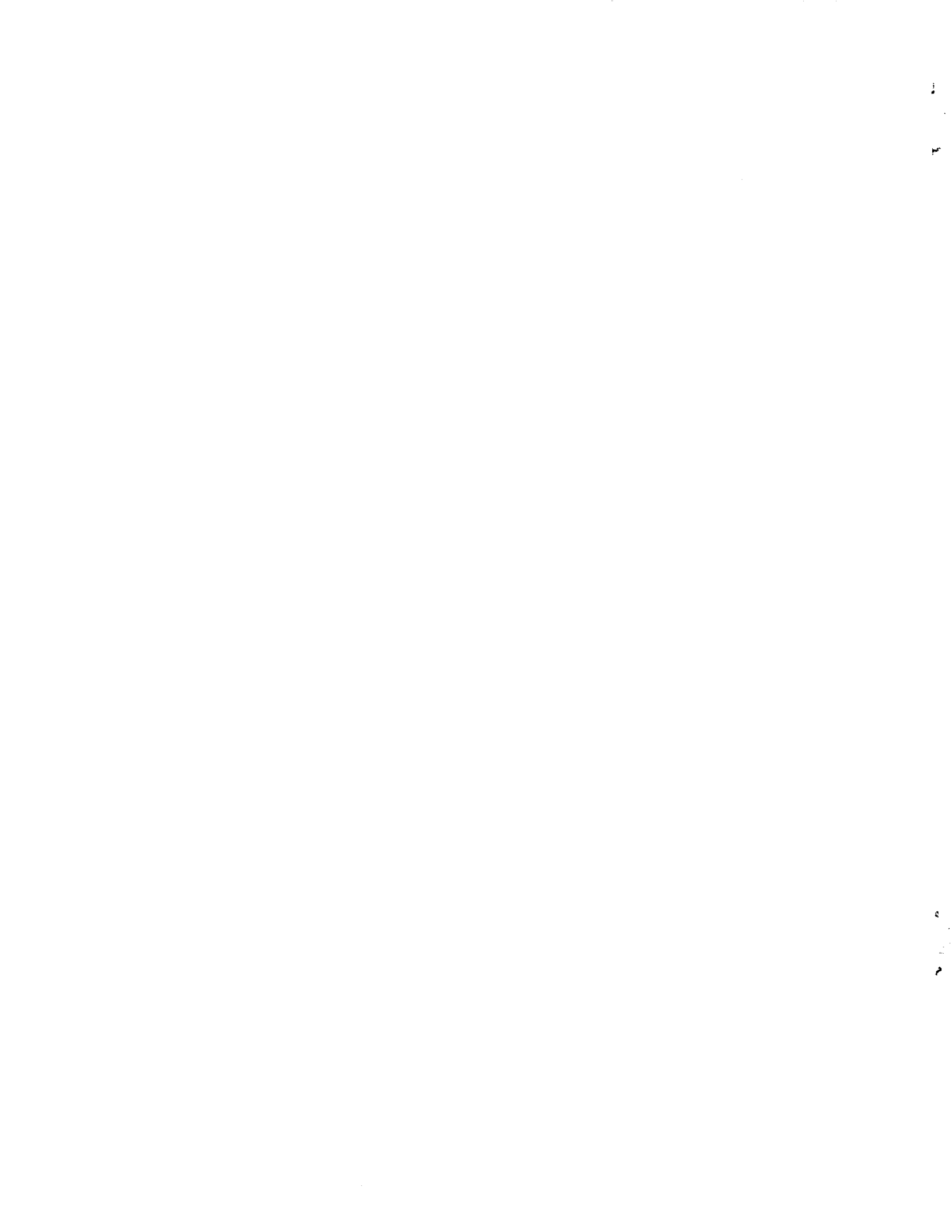
**A MODEL DESIGNED TO PREDICT THE  
MOTION OF OBJECTS TRANSLATED  
BY CLASSICAL BLAST WAVES**

**By**

**I. Gerald Bowen, Ray W. Albright,  
E. Royce Fletcher, and Clayton S. White**

**Approved by: R. L. CORSBIE  
Director  
Civil Effects Test Operations**

**Lovelace Foundation for Medical Education and Research  
Albuquerque, New Mexico  
January 1961**



## ABSTRACT

A theoretical model was developed for the purpose of predicting the motion of objects translated by winds associated with "classical" blast waves produced by explosions. Among the factors omitted from the model for the sake of simplicity were gravity and the friction that may occur between the displaced object and the surface upon which it initially rested. Numerical solutions were obtained (up to the time when maximum missile velocity occurs) in terms of dimensionless quantities to facilitate application to specific blast situations. The results were computed within arbitrarily chosen limits for blast waves with shock strengths from 0.068 to 1.7 atm (1 to 25 psi at sea level) for displaced objects with aerodynamic characteristics ranging from those of a human being to those of 10-mg stones and for weapon yields at least as small as 1 kt or as large as 20 Mt.

## ACKNOWLEDGMENTS

The authors wish to acknowledge helpful discussions with Sandia Corporation personnel in the Weapons Effects Department, especially in regard to the physics of the blast wave. Among those giving consultation were Mr. L. J. Vortman, Dr. M. L. Merritt, Dr. T. B. Cook, and Dr. C. D. Broyles.

Particular appreciation is expressed to Dr. Harold L. Brode of Rand Corporation for the blast-wave data that he supplied to us in the form of empirical equations derived from results computed from a point-source explosion model.

Computations necessary for the numerical solution of the equations of motion derived in this report were made possible through the cooperation of the Systems Analysis Department of Sandia Corporation. This department not only made available to us an electronic digital computer but also assisted in the preparation of a suitable program to accomplish the necessary computations. For this help we wish to thank Dr. W. W. Bledsoe, Dr. D. R. Morrison, Mrs. Pauline Van Delinder, and Mr. W. W. Whisler.

Also, appreciation is expressed to Lovelace Foundation personnel who assisted in the preparation of this report: Mr. Jerome Kleinfeld, Mr. Malcolm A. Osoff, and Mr. David W. Roeder for preparation of data for charts and tables; Mr. Robert A. Smith, Mr. Roy D. Caton, and Mr. George S. Bevil for preparation of illustrative material; Mrs. Isabell D. Benton, Mrs. Martina B. Smith, Mrs. Joanna Upthegrove, and Mrs. Frances E. Moore for editorial and secretarial assistance in preparation of the manuscript.

Lastly, the work reported here is a segment of that carried out on the biological effects of blast from bombs made possible through support by the Division of Biology and Medicine of the Atomic Energy Commission under contract with the Lovelace Foundation. The interest and encouragement of Dr. C. L. Dunham, Mr. R. L. Corsbie, Dr. H. D. Bruner, and Dr. J. F. Bonner, all of the Atomic Energy Commission, are gratefully acknowledged.

# CONTENTS

ABSTRACT . . . . .	5
ACKNOWLEDGMENTS . . . . .	6
CHAPTER 1 INTRODUCTION . . . . .	11
1.1 Objectives . . . . .	11
1.2 Scope and Limitations . . . . .	11
CHAPTER 2 ANALYTICAL PROCEDURE . . . . .	13
2.1 Nomenclature . . . . .	13
2.2 Equations of Motion . . . . .	14
2.2.1 Fundamental Concepts . . . . .	14
2.2.2 Time Correction . . . . .	14
2.2.3 Dimensional Analysis . . . . .	15
2.2.4 Approximation Solution . . . . .	15
2.3 Evaluation of Blast-wave Variables . . . . .	16
2.3.1 General Remarks . . . . .	16
2.3.2 Dynamic Pressure and Wind Velocity . . . . .	16
2.3.3 Overpressure vs. Time and Overpressure Impulse . . . . .	17
2.3.4 Duration Concepts . . . . .	18
2.3.5 Velocity of Propagation of the Pressure Disturbance . . . . .	18
CHAPTER 3 COMPUTATIONAL METHOD . . . . .	22
3.1 Scope of Computational Effort . . . . .	22
3.2 General Planning . . . . .	22
3.3 Step Size . . . . .	22
3.4 Machine Output . . . . .	24
3.5 Discussion of Error . . . . .	25
CHAPTER 4 RESULTS: COMPUTED MOTION PARAMETERS FOR OBJECTS DISPLACED BY CLASSICAL BLAST WAVES . . . . .	26
CHAPTER 5 INTERPRETATION OF RESULTS . . . . .	33
5.1 General Remarks . . . . .	33
5.2 Acceleration Coefficients for Various Objects . . . . .	33
5.3 Weapon Yield as a Blast Parameter . . . . .	36
5.4 Maximum Velocity and Corresponding Displacement . . . . .	36
5.5 Estimation of Maximum Velocity from Total Displacement . . . . .	43
5.6 Computed Velocity and Displacement for Particular Objects . . . . .	43
5.6.1 Interpolation of Alpha and Overpressure . . . . .	43
5.6.2 Velocity and Displacement Predicted for Man and for Glass Fragments . . . . .	43

# CONTENTS (Continued)

5.6.3	Predicted Maximum Velocities and Corresponding Displacements for 1-g Stones . . . . .	46
CHAPTER 6	DISCUSSION . . . . .	47
APPENDIX A	APPROXIMATION METHODS TO SUPPLEMENT THE COMPUTED RESULTS . . . . .	49
A.1	General Remarks . . . . .	49
A.2	Equations of Motion Applying for Short Times After Arrival of the Blast Wave . . . . .	49
A.3	Equations of Motion for Objects with Small Acceleration Coefficients . . . . .	50
A.4	Approximation Relations for Large Acceleration Coefficients . . . . .	52
A.5	Normalized Velocity vs. Distance for Missiles with Low Acceleration Coefficients . . . . .	54

## ILLUSTRATIONS

### CHAPTER 2 ANALYTICAL PROCEDURE

2.1	Shock Overpressure as a Function of the Ratio of Overpressure Impulse to Overpressure Duration . . . . .	19
2.2	Ratio of Duration of Wind to That of Overpressure as a Function of Shock Overpressure . . . . .	20

### CHAPTER 3 COMPUTATIONAL METHOD

3.1	Blast and Missile-motion Parameters vs. Time After Arrival of Blast Wave . . . . .	23
-----	--	----

### CHAPTER 5 INTERPRETATION OF RESULTS

5.1	Anthropometric Dummy Translation History, Obtained from Full-scale Weapon Test, Compared with That Predicted Using Various Values of Acceleration Coefficient and Computed Data . . . . .	35
5.2	Predicted Maximum Velocity as a Function of Acceleration Coefficient and Shock Overpressure (W = 1 kt) . . . . .	37
5.3	Predicted Displacement at Maximum Velocity as a Function of Acceleration Coefficient and Shock Overpressure (W = 1 kt) . . . . .	38
5.4	Predicted Maximum Velocity as a Function of Acceleration Coefficient and Shock Overpressure (W = 20 kt) . . . . .	39
5.5	Predicted Displacement at Maximum Velocity as a Function of Acceleration Coefficient and Shock Overpressure (W = 20 kt) . . . . .	40
5.6	Predicted Maximum Velocity as a Function of Acceleration Coefficient and Shock Overpressure (W = 1000 kt) . . . . .	41
5.7	Predicted Displacement at Maximum Velocity as a Function of Acceleration Coefficient and Shock Overpressure (W = 1000 kt) . . . . .	42
5.8	Relation Between Velocity and Displacement as a Function of Weapon Yield . . . . .	44
5.9	Relation Between Shock Overpressure and Yield for Various Values of Maximum Velocity and Displacement at Maximum Velocity . . . . .	45



# ILLUSTRATIONS (Continued)

## APPENDIX A APPROXIMATION METHODS TO SUPPLEMENT THE COMPUTED RESULTS

A.1	Relation Between Velocity, Displacement, and Time After Arrival of the Blast Wave . . . . .	51
A.2	Displacement at Maximum Velocity as a Function of Acceleration Coefficient for Various Values of Shock Overpressure . . . . .	53
A.3	Normalized Velocity vs. Normalized Displacement for Various Values of Acceleration Coefficient . . . . .	55

## TABLES

### CHAPTER 3 COMPUTATIONAL METHOD

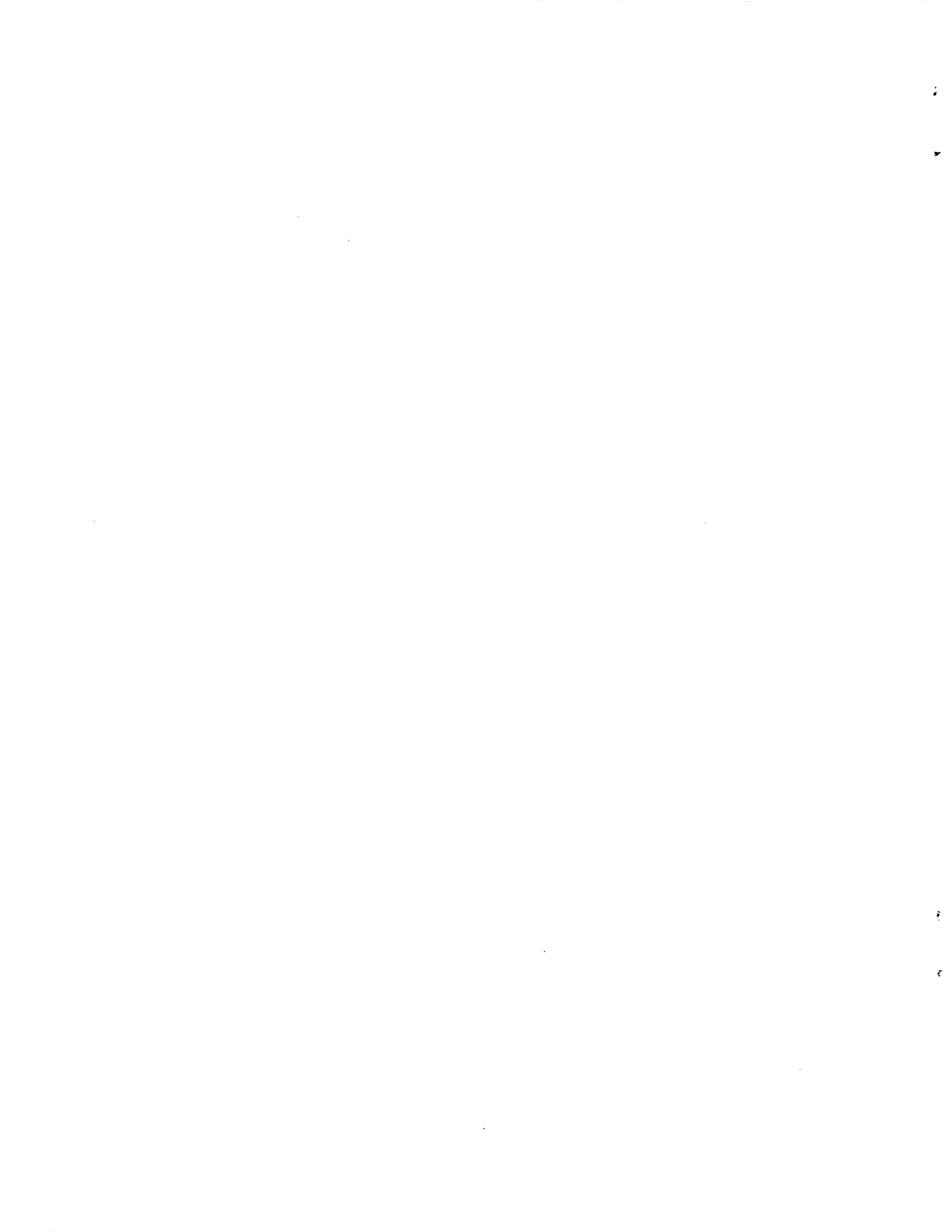
3.1	Incremental Values of the Independent Variable and Parametric Values for Which Computations Were Performed . . . . .	24
-----	--	----

### CHAPTER 4 RESULTS: COMPUTED MOTION PARAMETERS FOR OBJECTS DISPLACED BY CLASSICAL BLAST WAVES

4.1	Computed Motion Parameters for Objects Displaced by Classical Blast Waves . . . . .	27
-----	---	----

### CHAPTER 5 INTERPRETATION OF RESULTS

5.1	Typical Acceleration Coefficients . . . . .	34
-----	---	----



# Chapter 1

## INTRODUCTION

### 1.1 OBJECTIVES

During the 1955 and 1957 Test Operations at the Nevada Test Site, the masses and velocities of over 20,000 objects (window-glass fragments, stones, spheres, sticks, etc.) which were translated by nuclear-produced blast waves were experimentally determined,<sup>1-4</sup> along with a time-displacement history of an anthropometric dummy simulating man.<sup>5</sup> The availability of such a mass of data stimulated an analytical study calculated to arrive at a mathematical formulation capable of predicting the translation of objects by blast, particularly since this data offered an empirical fabric against which to test the success of the analytical effort.

The purpose of this report is to describe, step by step, the theoretical studies that have resulted in a mathematical model capable of predicting the motion of objects utilizing selected basic blast parameters. This model, however, is applicable only to those situations in which \*classical wave forms exist.

### 1.2 SCOPE AND LIMITATIONS

The applicability of the model itself has no well-defined limits; however, the numerical solutions that were obtained and are reported herein have been arbitrarily limited in scope. In general, the aim was to compute velocity, displacement, and acceleration as a function of time for objects ranging in size from a pea to man; these computations were to cover blast waves with shock overpressures from 1 to 25 psi (14.7-psi ambient pressure) and weapon yields from 1 kt to 20 Mt.

Another class of limitations is invoked not by the scope of the computations, but by the model itself. Formulation of a workable model was facilitated by the use of certain simplifying assumptions. These assumptions, which are discussed below, have not, in general, caused serious discrepancies between predicted velocities and those measured in the field operations, particularly in those situations where the blast wave was classical.†

As a practical approach, it was assumed first that the effect of surface friction was negligible. It has been observed that fairly large objects tend to be lofted when subjected to blast waves; the more intense the blast, the heavier the object that it is capable of lifting against gravity. Nonspherical objects could develop either positive or negative lift depending on their orientation to the wind. Thus, the validity of the no-friction assumption is dependent upon the strength of the blast wave, the object under consideration, its random orientation, and the nature of the surface over which translation occurs. It will be shown later that certain uses can be made of the data even for situations in which surface friction is a significant factor.

---

\*The term "classical blast wave" is used in this report to mean the typical wave not appreciably modified by terrain effects and possessing a well-defined shock front.

†A limited discussion of the agreement between predicted and measured velocities is made later in this report. A more complete treatment will be found in Ref. 3.

A second approximation made concerned the assumption that there was no gain or loss of energy as a result of the object's moving with or against gravity. The kinetic energy that is lost during lofting would be regained as the object fell to its original elevation, thus mitigating somewhat the error in the predicted motion.

Third, only the propelling force of the wind was considered. Another force that might have been included was that due to differences in overpressure between one side of the object and the other during passage of the shock front (diffractive loading). Since the bodies being considered were relatively small (up to the size of man), the classical blast wave would engulf the object very quickly and impart only a small momentum as a result of the overpressure itself.

Fourth, it was assumed that there was no change in the properties of an object which governed acceleration (area presented to the wind, drag coefficient, and mass) during the accelerative phase of displacement. For irregular, rigid objects that are nearly spherical, such as stones, this is a reasonable assumption. For objects that are obviously nonspherical or deformable, prediction of a range of velocities taking into account both maximum and minimum drag areas is often used. Another useful procedure is to employ the average drag area derived from the concept of random orientation.<sup>6</sup>

Fifth, no allowance was made for the fact that a displaced object may be moved to a lower overpressure region and thus be acted upon by correspondingly weaker blast winds. The results of the computations themselves seem to justify the neglect of this phenomenon. It will be shown that displaced objects receive a large percentage of their velocities in a relatively short distance over which the decay of the blast wave is small.

#### REFERENCES

1. I. Gerald Bowen, Allen F. Strehler, and Mead B. Wetherbe, Distribution and Density of Missiles from Nuclear Explosions, Operation Teapot Report, WT-1168, March 1956.
2. I. Gerald Bowen, Donald R. Richmond, Mead B. Wetherbe, and Clayton S. White, Biological Effects of Blast from Bombs. Glass Fragments as Penetrating Missiles and Some of the Biological Implications of Glass Fragmented by Atomic Explosions, Report AECU-3350, June 18, 1956.
3. I. Gerald Bowen et al., Secondary Missiles Generated by Nuclear-produced Blast Waves, Operation Plumbbob Report, WT-1468 (in preparation).
4. V. C. Goldizen, D. R. Richmond, and T. L. Chiffelle, Missile Studies with a Biological Target, Operation Plumbbob Report, WT-1470, January 1961.
5. R. V. Taborelli, I. G. Bowen, and E. R. Fletcher, Tertiary Effects of Blast-Displacement, Operation Plumbbob Report, WT-1469, May 22, 1959.
6. E. Royce Fletcher et al., Determination of Aerodynamic Drag Parameters of Small Irregular Objects by Means of Drop Tests, Civil Effects Test Operations, Report CEX-59.14 (in preparation).

## Chapter 2

### ANALYTICAL PROCEDURE

#### 2.1 NOMENCLATURE

The terminology used in this study is defined in this section. A lower-case letter is used to represent a quantity with dimensions. In general, the same letter is capitalized if the quantity is made dimensionless by an appropriate factor or factors. Thus, the dimensionless term is represented by its principle variable. The factors, or parameters, used to make quantities dimensionless invariably are constants for any given blast situation.

- $\alpha$  = acceleration coefficient =  $sC_d/m$
- $A = \alpha p_0 t_u^+ / c_0$
- $c_0$  = speed of sound in undisturbed air
- $C_d$  = drag coefficient of moving object
- $d$  = distance of travel of moving object
- $d_m$  = distance of travel of moving object when maximum velocity is reached
- $D = d / (t_u^+ c_0)$
- $I = \text{overpressure impulse} = \int_0^{t_p^+} P dt$
- $m$  = mass of moving object
- $p$  = overpressure or pressure in excess of  $p_0$
- $p_0$  = pressure of undisturbed air
- $p_s$  = maximum or shock overpressure
- $P = p/p_0$
- $P_s = p_s/p_0$ , shock overpressure in atmospheres
- $q = \text{dynamic pressure} = (1/2)\rho u^2$
- $q_s = \text{dynamic pressure at the shock front}$
- $Q = q/p_0$
- $Q_s = q_s/p_0$
- $\rho$  = air density
- $s$  = area presented to wind by moving object
- $t$  = time after arrival of blast wave
- $t_p^+ = \text{duration of positive pressure phase of blast wave}$
- $t_u^+ = \text{duration of winds in the direction of propagation of the blast wave}$
- $T = t/t_p^+$
- $u$  = velocity of the air
- $U = u/c_0$
- $v$  = velocity of the moving object
- $v_m = \text{maximum velocity of moving object}$
- $V = v/c_0$
- $\dot{v} = \text{acceleration of moving object}$
- $\dot{V} = \dot{v}t_u^+ / c_0$
- $W = \text{weapon yield in kilotons}$
- $\dot{x} = \text{velocity of propagation of the pressure disturbance}$

$$\begin{aligned}\dot{\bar{X}} &= \dot{x}/c_0 \\ Z &= t/t_u^+\end{aligned}$$

NOTE: Any variable that is underlined indicates the average value taken over a particular time interval.

## 2.2 EQUATIONS OF MOTION

### 2.2.1 Fundamental Concepts

Newton's second law of motion can be stated as

$$\text{Force} = m \frac{dv}{dt}$$

and the drag force on a moving object is

$$\text{Force} = \frac{1}{2} \rho (u - v)^2 s C_d$$

since the net wind moving past the object is  $(u - v)$ . Combining the above equations and solving for  $dv$ , we obtain

$$dv = \rho \frac{(u - v)^2}{2} \frac{s C_d}{m} dt \quad (2.1)$$

It was convenient to isolate and label the physical parameters that involve the moving object in Eq. 2.1.

$$\frac{s C_d}{m} = \alpha \quad (2.2)$$

Now,  $\alpha$  can be called "acceleration coefficient" since it completely describes the object in so far as the computation of velocity vs. time is concerned. Thus, two objects possessing the same value of  $\alpha$ , regardless of dissimilarity of shape, size, and mass, would experience the same increase in velocity if exposed to the same or similar blast waves.

### 2.2.2 Time Correction

Since the moving object, or missile, travels along with the blast wave, the time during which it is exposed to blast winds is longer the higher its velocity is in relation to the velocity of propagation of the pressure disturbance and associated winds. Consider a small segment of the blast wave of length  $dx$  where the air-particle density and velocity are approximately constant. If this segment moves with a velocity  $\dot{x}$ , then

$$dx = \dot{x} dt$$

where  $dt$  is the time required for the segment  $dx$  to pass a fixed point. Similarly, the velocity of propagation of a blast-wave segment past a missile that itself is moving at velocity  $v$  is  $(\dot{x} - v)$ , and

$$dx = (\dot{x} - v) dt'$$

where  $dt'$  is the time required for the blast segment to pass the missile. By eliminating  $dx$  between the above equations, we obtain

$$dt' = dt \frac{\dot{x}}{\dot{x} - v} \quad (2.3)$$

Combining Eqs. 2.1 and 2.2 and substituting the corrected time  $dt'$  of Eq. 2.3 for  $dt$ , we obtain

$$dv = \frac{1}{2} \rho \alpha (u - v)^2 \frac{\dot{x}}{(\dot{x} - v)} dt \quad (2.4)$$

It was more convenient to work with dynamic pressure,  $q = (1/2) \rho u^2$ , than with air density. For this reason Eq. 2.4 was modified to

$$dv = q \alpha \left( \frac{u - v}{u} \right)^2 \frac{\dot{x}}{(\dot{x} - v)} dt \quad (2.5)$$

### 2.2.3 Dimensional Analysis

The blast-wave variables in Eq. 2.5 are determined as a function of time by four parameters: (1) shock overpressure,  $p_s$ ; (2) ambient pressure,  $p_0$ ; (3) duration of the positive winds,  $t_u^+$ ; and (4) speed of sound in the undisturbed air,  $c_0$ . Computations were made for particular values of shock overpressure in atmospheres,  $P_s = p_s/p_0$ . The last three parameters, however, were used to make the variables in Eq. 2.5 dimensionless. The obvious advantage of this procedure is that computed values of missile velocity, distance of travel, and acceleration can be modified after the computations have been made to fit any blast situation defined by  $p_0$ ,  $t_u^+$ , and  $c_0$ .

The variables of Eq. 2.5 were made dimensionless through the application of the following algebraic operations: (1) both sides of the equation were divided by  $c_0$ , (2) the numerators and the denominators of the two fractions were divided by  $c_0$ , (3)  $\alpha$  was multiplied by  $p_0$  and  $q$  was divided by  $p_0$ , and (4)  $t$  was divided by  $t_u^+$  and  $\alpha$  was multiplied by  $t_u^+$ .

After these operations have been performed, Eq. 2.5 becomes

$$d\left(\frac{v}{c_0}\right) = \left(\frac{q}{p_0}\right) \left(\frac{\alpha p_0 t_u^+}{c_0}\right) \left[\frac{(u/c_0) - (v/c_0)}{u/c_0}\right]^2 \left[\frac{\dot{x}/c_0}{(\dot{x}/c_0) - (v/c_0)}\right] d\left(\frac{t}{t_u^+}\right) \quad (2.6)$$

and, after appropriate substitutions (see Sec. 2.1, Nomenclature)

$$dV = QA \left(\frac{U - V}{U}\right)^2 \frac{\dot{X}}{\dot{X} - V} dZ \quad (2.7)$$

Two additional quantities are used in dimensionless form, distance of travel and acceleration. Since both are functions of velocity and time, their dimensionless forms are determined by dimensionless velocity and time. Thus

$$D = VZ = \frac{v}{c_0} \frac{t}{t_u^+} = \frac{d}{c_0 t_u^+} \quad (2.8)$$

and

$$\dot{V} = \frac{V}{Z} = \frac{vt_u^+}{c_0 t} = \frac{\dot{v}t_u^+}{c_0} \quad (2.9)$$

### 2.2.4 Approximation Solution

The explicit expressions of  $Q$ ,  $U$ , and  $\dot{X}$  as a function of time for a particular blast wave are very cumbersome. Added to this difficulty is the fact that the variable  $V$  cannot be separated from the time-dependent variables (see Eq. 2.7). Hope for a complete mathematical solution was soon abandoned.

A stepwise solution was then attempted which would permit the blast parameters to be held constant for small increments of time but would allow the missile velocity to vary as a nonlinear function of time. So that a simple mathematical integration can be accomplished, the

time-correction term,  $\dot{X}/(\dot{X} - V)$ , was not included. Thus

$$\int_{V_0}^{V_0+\Delta V} \frac{dV}{(\underline{U} - V)^2} = \underline{QA} \int_{Z_0}^{Z_0+\Delta Z'} dZ \quad (2.10)$$

where  $V_0$  and  $Z_0$  are the velocity and time, respectively, at the beginning of the time period and  $\Delta V$  is the change in velocity in time  $\Delta Z'$ . Underlined  $U$  and  $Q$  indicate average values over the time  $\Delta Z'$ .

Integration of Eq. 2.10 and substitution of limits yields

$$\frac{1}{\underline{U} - V_0 - \Delta V} - \frac{1}{\underline{U} - V_0} = \underline{QA} \Delta Z' \quad (2.11)$$

The average missile velocity during the time period  $\Delta Z'$  is  $[V_0 + (1/2)\Delta V]$ . Thus the time-correction term (see Eq. 2.3) expressed in dimensionless incremental form is

$$\Delta Z' = \Delta Z \frac{\dot{X}}{\dot{X} - V_0 - (1/2)\Delta V} \quad (2.12)$$

Eliminating  $\Delta Z'$  between Eqs. 2.11 and 2.12 and solving for  $\Delta V$ , the following is obtained

$$\Delta V = e + f - \sqrt{e^2 + 2fg + f^2} \quad (2.13)$$

where  $e = \underline{X} - V_0$   
 $f = \underline{AQ} (\underline{U} - V_0) \dot{X} (\Delta Z / \underline{U}^2)$   
 $g = \dot{X} - \underline{U}$

The velocity at the end of any step is the summation of the  $\Delta V$ 's computed from the beginning of the integration.

Incremental distance,  $\Delta D$ , was computed by the following:

$$\Delta D = [V_0 + (1/2)\Delta V] \Delta Z' \quad (2.14)$$

where  $V_0$  refers to the velocity at the beginning of the step.  $\Delta Z'$  is defined in Eq. 2.12.

Evaluation of acceleration ( $\dot{V} = dV/dZ$ ) presented little difficulty since integration was not involved. Furthermore, the time-correction term was not necessary because, by definition,  $\dot{V}$  is the instantaneous time rate of change in velocity. Thus, the following equation was formed from Eq. 2.7:

$$\dot{V} = \frac{dV}{dZ} = QA \left( \frac{U - V}{U} \right)^2 \quad (2.15)$$

## 2.3 EVALUATION OF BLAST-WAVE VARIABLES

### 2.3.1 General Remarks

A particular classical blast wave can be completely defined mathematically by the parameters of shock strength ( $p_s/p_0$ ), duration, and either the velocity of sound or the temperature for ambient conditions. Secondary-missile computations were made for selected values of shock strength, each of which is applicable to any value of duration (and thus bomb yield) or ambient sound velocity between wide limits.

### 2.3.2 Dynamic Pressure and Wind Velocity

Although dynamic pressure (from which wind may be computed) has been measured in ac-



tual blast situations, values computed from theoretical considerations were used in this study. The reason for this was both the higher reliability and the greater facility for numerical treatment of the computed parameters over the measured ones. Of the several studies made of the blast wave, those made by Harold L. Brode of Rand Corporation<sup>1,2</sup> were found to be most useful for the present study. The equations<sup>3</sup> listed below are empirical relations determined by fitting curves to computed blast data. In terminology consistent with the present study, dynamic pressure as a function at shock overpressure and time is given by

$$Q = Q_s (1 - Z) [J e^{-\gamma Z} + K e^{-\delta Z}] \quad (2.16)$$

where  $Q_s = \left( \frac{2.5 P_s^2}{7 + P_s} \right) \left( \frac{1 + 2 \times 10^{-8} P_s^4}{1 + 10^{-8} P_s^4} \right)$   
 $J = 1.186 P_s^{1/3}$  for  $P_s < 0.6$   
 $J = 1$  for  $0.6 \leq P_s \leq 1.0$   
 $J = (10^4 P_s^{-1/4}) / (10^4 + P_s^2)$  for  $P_s > 1$   
 $K = 1 - J$   
 $\gamma = (1/4) + 3.6 P_s^{1/2}$   
 $\delta = (7 + 8 P_s^{1/2}) + 2 P_s^2 / (240 + P_s)$

The relation for wind, or particle, velocity is

$$U = U_s (1 - Z) e^{-\nu Z} \quad (2.17)$$

where  $U_s = (P_s) / (1 + P_s^{1/2})$   
 $\nu = P_s^{1/3} + 0.0032 P_s^{3/2}$

### 2.3.3 Overpressure vs. Time and Overpressure Impulse

Overpressure as a function of time does not enter directly into the computation of secondary-missile behavior; nevertheless, it seems appropriate to consider this relation since it is the most commonly measured parameter of the real blast wave. Thus, overpressure-time can be considered to be the bridge between secondary-missile field data and the computed data resulting from the present study.

The following overpressure-time relation was obtained from Brode:<sup>1-3</sup>

$$P = P_s (1 - T) (a e^{-iT} + b e^{-jT}) \quad (2.18)$$

where  $a = \frac{2.282 (8 + P_s)}{27.658 + P_s + 1.2 P_s^2 + 0.007 P_s^3} + 0.23$   
 $b = 1 - a$   
 $i = \sqrt{\frac{P_s}{1 + 0.1 P_s}} + \frac{1.5 P_s^2}{1500 + P_s^{3/2}}$   
 $j = 9 + 1.4 P_s$

Pressure instrumentation used in field work often produces a more accurate measurement of overpressure impulse than of shock overpressure. Indeed, an improved estimate of shock overpressure can be made by making use of the impulse relation described below.

Overpressure impulse is defined as

$$I = \int_0^{t_p^+} P dt \quad (2.19)$$

However, to facilitate integration of Eq. 2.18 in terms of normalized time, the following relation was used:

$$T = t/t_p^+ \quad (2.20)$$

thus,

$$dt = t_p^+ dT \quad (2.21)$$

A combination of Eqs. 2.19 and 2.21 gives

$$I = t_p^+ \int_0^1 P dT \quad (2.22)$$

Integration of Eq. 2.18 in the manner indicated by Eq. 2.22 yields the following:

$$I = P_s t_p^+ \left[ \frac{a}{e^2} (e^{-i} + i - 1) + \frac{b}{f^2} (e^{-j} + j - 1) \right] \quad (2.23)$$

Figure 2.1, a plot of  $P_s$  in atmospheres as a function of  $I/t_p^+$  also in atmospheres, illustrates this relation graphically. This plot can be thought of as defining the "shape factor" of the overpressure-time curve as a function of maximum overpressure. If impulse,  $I$ , and duration,  $t_p^+$ , are measured by suitable instrumentation, then a value of shock overpressure can be determined from the curve shown in this figure.

### 2.3.4 Duration Concepts

(a) *Positive-overpressure Duration.* To evaluate the computed motion parameters for a particular yield, it is obviously necessary to know the duration of the blast wave (identified by peak or shock overpressure) of interest. For this purpose the durations computed from theoretical considerations for free-air conditions, such as those by Brode, are of little value since the complex effects of surface reflections are not considered. Thus, the semiempirical relations presented in Chap. 3 of *The Effects of Nuclear Weapons*<sup>4</sup> were used to define overpressure duration as a function of yield, overpressure, ambient pressure, and the speed of sound. Using data for both the surface burst and the "typical air burst," the following mathematical expression was derived

$$\log t_p^+ = 5.7995 + (1/3) \log W - 0.2957 \log p_s - 0.0376 \log p_0 - \log c_0 \quad (2.24)$$

where  $t_p^+$  = duration of positive overpressure in milliseconds

$W$  = yield in kilotons

$p_s$  = shock overpressure in pounds per square inch

$p_0$  = ambient pressure in pounds per square inch

$c_0$  = velocity of sound in the undisturbed air in feet per second

The above equation reflects data for the surface burst for shock overpressure (sea-level conditions) from 1.68 to 36.7 psi and for the "typical air burst" from 1.86 to 19.7 psi.

(b) *Overpressure vs. Wind Duration.* Instrumentation used in past weapons tests was not refined enough to establish a relation between overpressure and wind duration. However, the theoretical work quoted above has established such a relation. Figure 2.2, derived from Brode's work,<sup>1,3</sup> presents the ratio of the wind duration to the pressure duration for overpressures up to 3 atm (44.1 psi at sea level). It is apparent from this chart that for the higher overpressures air-particle inertia has the effect of sustaining positive winds for an appreciable time after the overpressure has become negative.

### 2.3.5 Velocity of Propagation of the Pressure Disturbance

It has been shown that it is necessary to know the velocity of propagation of the pressure disturbance in order to compute the motion of objects displaced by blast waves. An easily evaluated relation<sup>5</sup> that was used for this purpose is:

$$\dot{X} = \frac{3}{5} U + \sqrt{1 + \left(\frac{3}{5} U\right)^2} \quad (2.25)$$

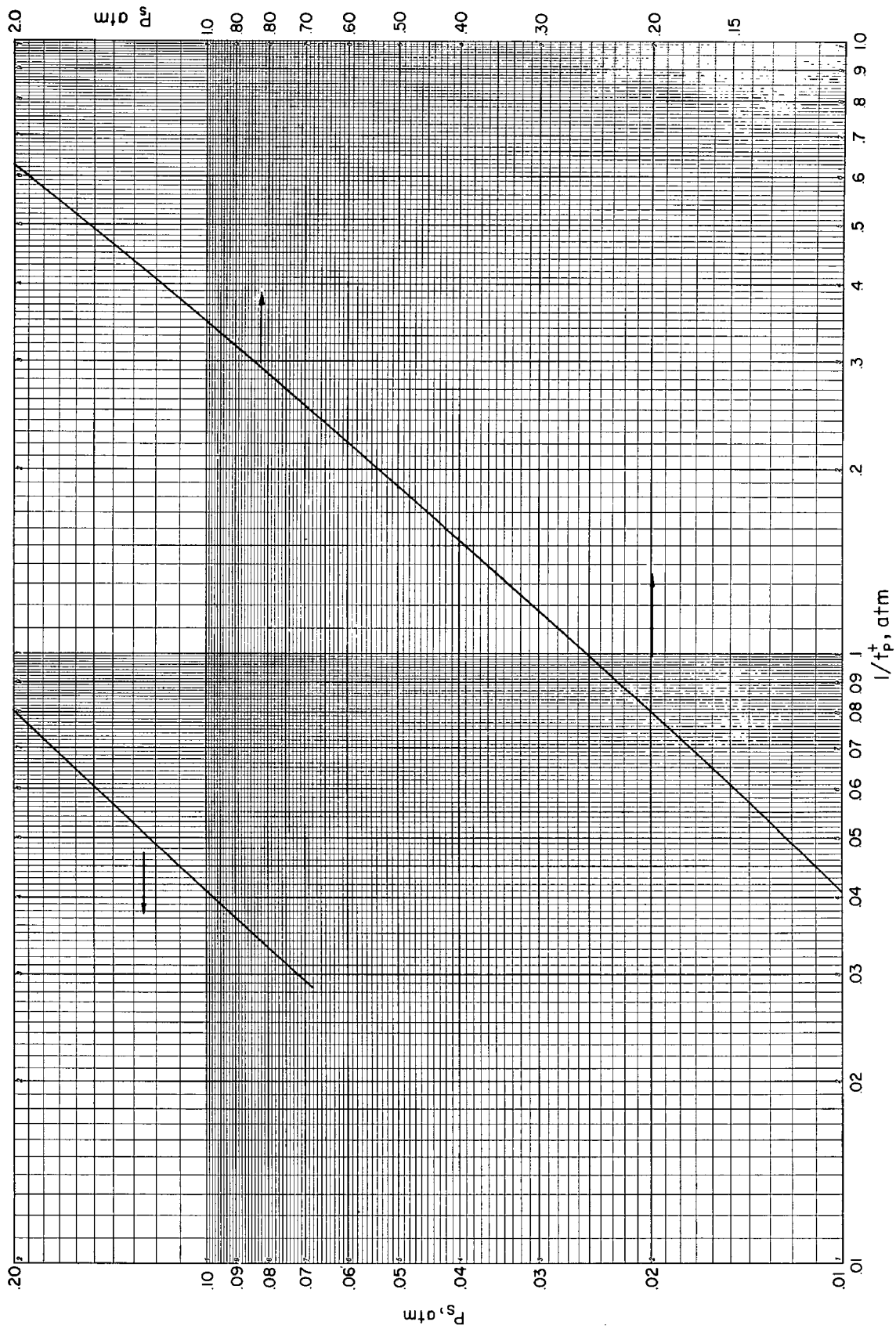


Fig. 2.1 — Shock overpressure as a function of the ratio of overpressure impulse to overpressure duration.

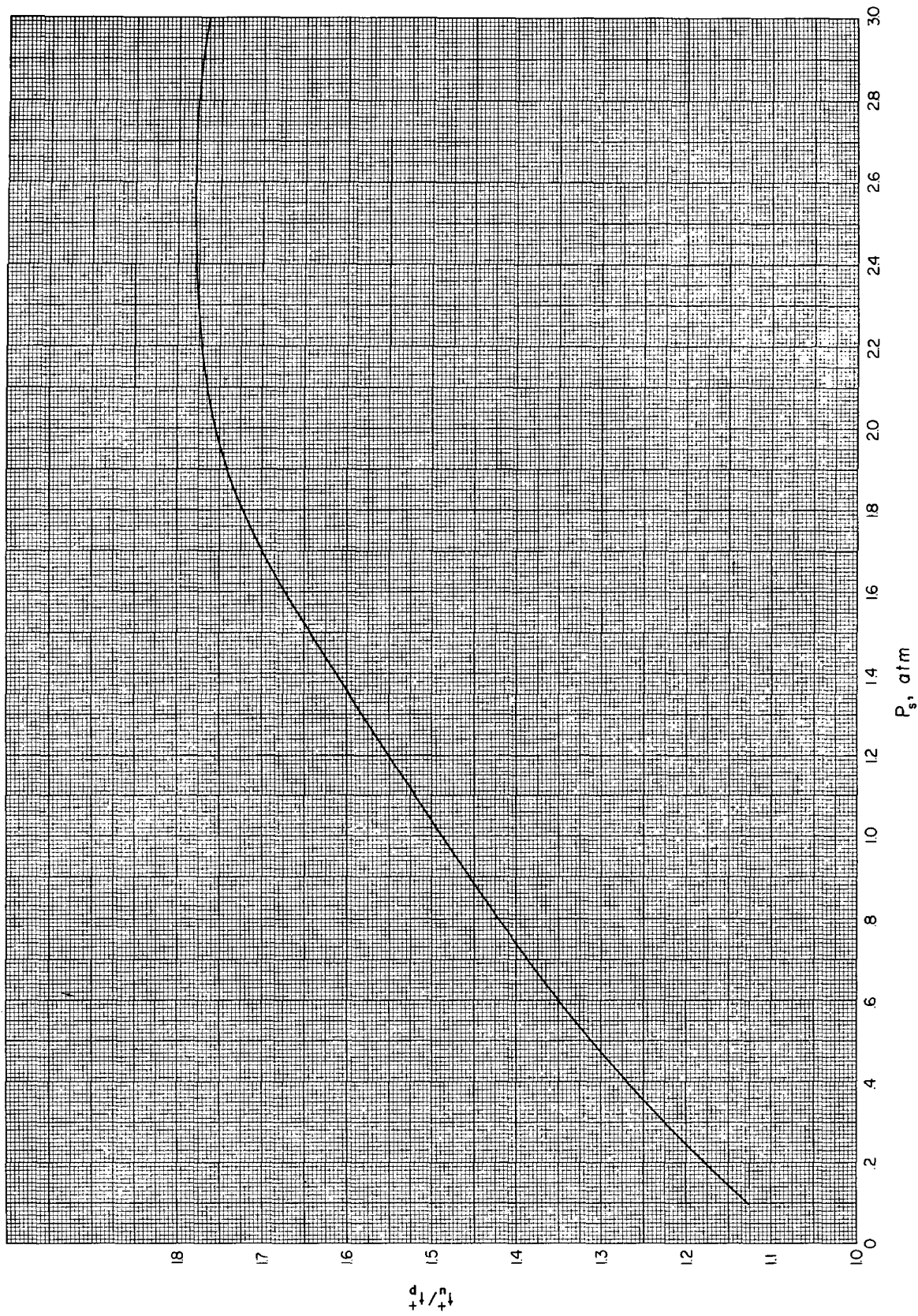


Fig. 2.2—Ratio of duration of wind to that of overpressure as a function of shock overpressure.

Two objections might be raised to the use of the above equation for the purposes of this study. First, it applies strictly to the speed of propagation of the shock front, not to pressure regions behind the front. Second, it was derived for nondivergent flow; whereas the present study applies to divergent flow. In spite of these limitations, the relation was found to be in reasonable agreement with work done by Brode<sup>1,2</sup> as quoted in Sec. 2.3.2.

This, added to the fact that  $X$  appears only in the time-correction term (see Eq. 2.7), whose effect on the computed value of  $dV$  is second order, probably justifies its use in the present context.

#### REFERENCES

1. Harold L. Brode, Numerical Solutions of Spherical Blast Waves, *J. Appl. Phys.*, 26: 766-775 (June 1955).
2. Harold L. Brode, Point Source Explosion in Air, Report AECU-3517, The Rand Corporation, Dec. 3, 1956.
3. Harold L. Brode, personal communication.
4. Samuel Glasstone (Ed.), *The Effects of Nuclear Weapons*, Superintendent of Documents, U. S. Government Printing Office, Washington, D. C., June 1957.
5. Ascher H. Shapiro, *The Dynamics and Thermodynamics of Compressible Fluid Flow*, Vol. 2, p. 1001, Ronald Press Company, New York, 1954.

## Chapter 3

### COMPUTATIONAL METHOD

#### 3.1 SCOPE OF COMPUTATIONAL EFFORT

Because computations were made in terms of dimensionless quantities, it was necessary to use only two independent variables: (1) the acceleration-coefficient numeric\* ( $A = \alpha p_0 t_u^+ / c_0$ ) containing acceleration coefficient, ambient pressure, speed of sound, and duration of positive winds (yield dependent) and (2) the shock-overpressure numeric ( $P_s = p_s / p_0$ ), which also involves the ambient pressure. Thus, five independent variables, one describing the object displaced and four describing the blast wave, were effectively reduced to two. It should be pointed out that the shock-overpressure numeric (along with the duration variable) represents or defines three other blast variables that are actually used in the computations; namely, dynamic-pressure numeric ( $Q$ ), wind numeric ( $U$ ), and propagation-velocity numeric ( $\dot{X}$ ), all of which are functions of the time numeric ( $Z = t/t_u^+$ ).

Thus, for computational purposes, it was necessary to set limits only on  $A$  and  $P_s$ . Consistent with the scope of the problem stated in Sec. 1.2, the limits arbitrarily set for  $A$  were 0.1 to 9000 and for  $P_s$  from 0.068 to 1.7 (1 psi to 25 psi for sea-level ambient pressure). Computations were made for 15 values of  $P_s$  within the stated range, and associated with each of these were 11 values of  $A$  (see Table 3.1, columns I and II), making a total of 165 complete numerical integrations.

#### 3.2 GENERAL PLANNING

Figure 3.1 illustrates some of the considerations in planning for numerical solutions of the mathematical model. This plot shows the pertinent blast variables in dimensionless form as functions of the time numeric ( $T = t/t_p^+$ ) for a 0.5-atm blast wave. Also shown on this plot are velocity ( $V = v/c_0$ ) and displacement ( $D = d/t_u^+ c_0$ ) computed for an object with an acceleration coefficient ( $A = \alpha p_0 t_u^+ / c_0$ ) of 30. It should be noted that all plotted quantities change most rapidly at early times. This means that a stepwise solution should be started using small time increments, these to be lengthened as the solution progresses. Also of interest on this chart is the  $U'$  curve, which represents the wind numeric at the position of the moving object rather than at a fixed position. At  $T = 0.5$ , missile velocity was equal to that of the wind, and so the integration was stopped. Sixty-two steps were taken to arrive at the solution shown here.

#### 3.3 STEP SIZE

As shock overpressures increase, the rate of decay of the blast variables from shock values also increases. For mean-value assumptions (i.e., the assumption that the variable is constant with a value equal to the mean over a specified time increment) to be equally valid for

---

\*Numeric is used here to designate a dimensionless quantity.

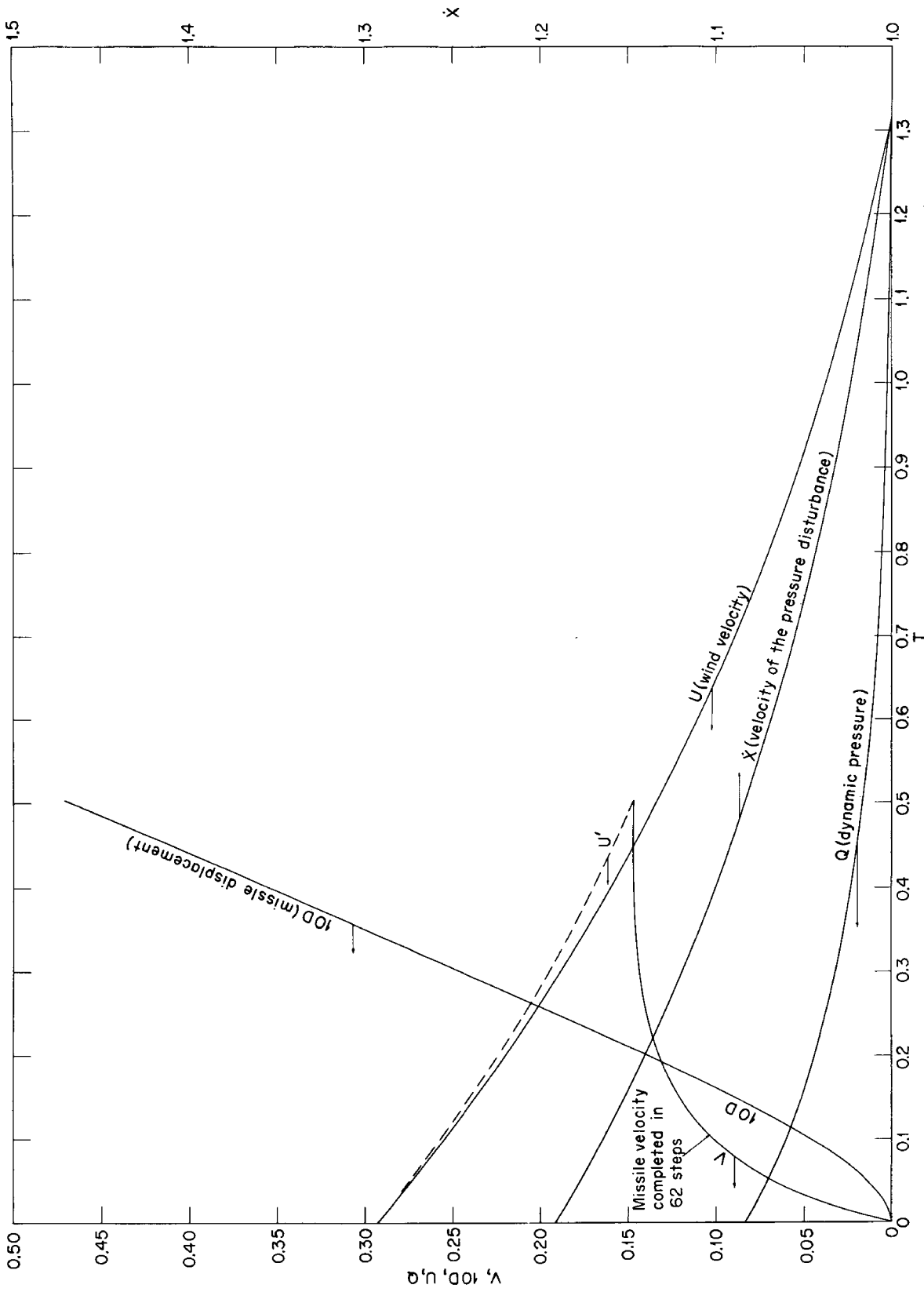


Fig. 3.1—Blast and missile-motion parameters vs. time after arrival of blast wave computed for  $p_s = 0.5$  atm,  $A = 30$  (all quantities dimensionless).  $Q$ ,  $U$ , and  $\dot{X}$  curves represent blast parameters as they would be measured at the point of origin of the missile. The  $U'$  curve represents the wind velocity existing at the location of the moving missile indicated by the displacement ( $D$ ) curve.

TABLE 3.1—INCREMENTAL VALUES OF THE INDEPENDENT VARIABLE AND PARAMETRIC VALUES FOR WHICH COMPUTATIONS WERE PERFORMED

$P_s$	I	II	III	IV
	$t_p^+/t_u^+$	A	$\Delta T^*$	$T_j^\dagger$
0.068	0.900	0.1	0.0001	0.002
0.10	0.885	0.3	0.0002	0.004
0.15	0.875	1	0.0003	0.008
0.20	0.855	3	0.0004	0.015
0.25	0.840	10	0.001	0.030
0.30	0.835	30	0.002	0.060
0.35	0.805	100	0.003	0.120
0.40	0.793	300	0.005	0.250
0.50	0.760	1000	0.007	0.500
0.60	0.740	3000	0.010	0.750
0.70	0.720	9000	0.025	1.000
0.80	0.710		0.050	Final
1.00	0.675		0.100	
1.30	0.635			
1.70	0.585			

\*Ten steps of each  $\Delta T$  were used starting with  $\Delta T = 0.001$ . See Sec. 3.3 for an explanation of first four values of  $\Delta T$ .

$\dagger T_j$  = times for which computed results were printed out.

high overpressures, the time increments should be correspondingly decreased. Noting that the ratio of overpressure duration to wind duration decreases for increasing overpressures (see Table 3.1, column I) suggested the use of a set of time increments in  $T$  constant for all solutions. The  $\Delta Z$  values computed for each overpressure (using  $\Delta Z = t_p^+/t_u^+ \Delta T$ ) then decrease as desired for the higher overpressure blast waves.

The first computation in each integration series was made for a time increment,  $\Delta T$ , equal to 0.001. If the velocity  $V$  so computed was greater than 0.1, the solution was discarded; then  $\Delta T$  values of 0.0001, 0.0002, 0.0003, and 0.0004 were used, in turn, and  $T = 0.001$  was arrived at in four steps. Succeeding steps, gradually increasing in size, were then taken until the end of the integration (see Table 3.1). If the initial step,  $\Delta T = 0.001$ , yielded a velocity less than 0.1, the integration proceeded from there without the use of the shorter steps.

The shortest integration, using the system described above, required 14 steps; this was for  $P_s = 1.7$ ,  $A = 9000$ . In general, the number of steps required increased as  $A$  decreased; e.g., 75 steps were required for  $A = 3.0$  and  $P_s = 0.068$  and 81 steps were required for  $A = 0.1$  and  $P_s = 1.7$ .

### 3.4 MACHINE OUTPUT\*

Since printing out results at the end of each step would have slowed the computation considerably and also would have produced much more information than could have been utilized, it was decided to limit the output of intermediate results to those necessary for the preparation of accurate plots. Because of the time-correction term (see Sec. 2.2.2), time at the end of any particular step was different for each set of conditions. For simplicity in monitoring results and ease of plotting time histories, it was convenient to program output at a set of preselected time (see Table 3.1, column IV). Thus, it was necessary to program the computer to interpolate (linearly) the computed results between time steps to the times selected for print-out.

Special problems arose in the determination of the final values of the computed results; i.e., the values occurring at the time when missile velocity and wind velocity were identical.

\*The computer, a CRC-102A, was generously made available by Sandia Corporation.



Since missile velocity changes very slowly near the end of the accelerative phase, it was sufficiently accurate to take final or maximum missile velocity to be that computed for the first step where it equaled or exceeded the wind velocity. However, it was necessary to obtain the time at which this occurred by interpolating the wind values to a time when they equaled maximum missile velocity. Making use of this time, displacement at maximum velocity could then be computed. Final acceleration was always, of course, zero.

### 3.5 DISCUSSION OF ERROR

The usable word length of the computer was 36 binary digits or the equivalent of 9 decimal digits of input or output. The fixed-point fractional mode of operation required careful scaling of all magnitudes (primarily because of the large range of the parameter A) so that sufficient significance be retained without the need for rescaling. Binary scaling proved adequately conservative in the attainment of this objective.

Approximations for square roots and cube roots were obtained with accuracy greater than eight decimal places, and the exponential approximation is reported to be accurate to  $\pm 2$  in the seventh decimal place. (Cube roots were obtained by the Newton-Raphson method,<sup>1</sup> and the exponential, by the rational polynomial approximation.<sup>2</sup>)

Blast-wave parameters were evaluated from empirical equations that were derived by fitting curves to computed data obtained from a blast-wave model.<sup>3,4</sup> Although Brode did not make a definite statement regarding the over-all accuracy of the blast model, he did indicate some deviation of the empirical equations from the computed data. From this it can be surmised that computations involved in the present problem were carried out as accurately as was warranted by the accuracy of the input blast data as well as by the probity of the missile model itself (see Sec. 1.2).

It is noteworthy that computed missile velocity becomes stable by virtue of the number of steps involved in each integration; i.e., if for some reason computed missile velocity at the end of a particular step is too low, the net wind velocity ( $U - V$ ) used in the next step will be correspondingly high, thereby tending to compensate for the original error. As a consequence the final solution is not extremely sensitive to the magnitude of the time increments so long as, within any particular solution, the steps are sufficiently numerous for the compensatory effect to be realized before the computation ends.

### REFERENCES

1. J. B. Scarborough, *Numerical Mathematical Analysis*, pp. 192-194, Johns Hopkins Press, Baltimore, Md., 1955.
2. C. Hastings, Jr., *Approximations for Digital Computers*, Princeton University Press, Princeton, N. J., 1955.
3. Harold L. Brode, Numerical Solutions of Spherical Blast Waves, *J. Appl. Phys.*, 26: 766-775 (June 1955).
4. Harold L. Brode, Point-source Explosion in Air, Report AECU-3517, The Rand Corporation, Dec. 3, 1956.

## Chapter 4

### RESULTS: COMPUTED MOTION PARAMETERS FOR OBJECTS DISPLACED BY CLASSICAL BLAST WAVES

The results of the 153 numerical integrations are presented in Table 4.1 in terms of the dimensionless parameters. Each integration was made for a specific combination of over-pressure (P) and acceleration coefficient (A). Values of missile velocity (V), distance of travel (D), and missile acceleration (V) are given for 13 times during the accelerative phase of missile displacement. Numbers appearing in parenthesis after V, D, and V are scaling factors indicating the number of places the decimal point has been moved to the right. Consider, for example, the data tabulated for  $P = 0.10$  and  $A = 1000$  at  $T = 0.120$ . In this instance  $V(6)$  is read as 55677, and thus  $V = 0.055677$ .

At  $T = 0$ , the time of arrival of the blast wave, velocity and displacement are zero, but acceleration is maximum. "T = Final" is defined as the time after arrival of the blast wave when missile velocity is maximum and acceleration is zero. The displacement (D) tabulated under "Final" is defined as the total displacement of the object at the instant when the velocity is maximum. The actual time when maximum velocity is attained appears in the last column under "T<sub>final</sub>."

It should be noted that the time measurements used in this table are normalized with respect to the duration of the positive pressure phase. Since the duration of positive winds is longer than that of the positive pressure, T<sub>final</sub> values are sometimes greater than unity. The exact value of T<sub>final</sub> is, of course, the time when the missile velocity equals the wind velocity.

Examples of uses of the tabulated data along with various plots are given in Chap. 5.















## Chapter 5

### INTERPRETATION OF RESULTS

#### 5.1 GENERAL REMARKS

The motion parameters of secondary missiles computed in the present study can be used in many different ways. The purpose of this chapter is to point out a few analytical techniques that have been found useful. Although the treatment is not exhaustive, such practical subjects as weapon scaling, acceleration coefficients, and interpolation techniques are discussed. In addition, samples of computed missile data are shown in graphic form.

#### 5.2 ACCELERATION COEFFICIENTS FOR VARIOUS OBJECTS

Acceleration coefficient has been defined as the product of the area presented to the wind by an object and its drag coefficient divided by its mass. To vivify the meaning of the computed results, it is necessary to relate values of acceleration coefficient to real objects. For this purpose Table 5.1 (based on Refs. 1-3) was prepared.

In regard to the acceleration coefficient for man, it is evident from these data that position with respect to the wind is quite important. Change of position during translation, as well as surface-friction effects, serves to complicate any attempt at an exact analysis. With respect to this problem, it is useful to note the results of an experiment reported by Taborelli et al.<sup>4</sup> in which anthropometric dummies, weighing 169 lb dressed and having a height of 5 ft 9 in., were used in connection with full-scale weapons tests. In one instance a dummy was placed on a concrete ramp standing with its back to the oncoming blast wave. The blast parameters at this location were: maximum overpressure 5.3 psi, ambient pressure 13.3 psi, duration of positive pressure 0.964 sec, and the velocity of sound in the ambient air 1120 ft/sec. Partial results of the motion picture analysis shown in Fig. 5.1 indicate that the dummy was accelerated to 21.4 ft/sec in 0.5 sec after having been displaced about 8 ft. By this time the dummy's position, which was initially vertical, had become horizontal with the head toward the oncoming blast wave (see chart at top of Fig. 5.1). Also shown on this figure are predicted velocity-time histories for various values of acceleration coefficient. It is interesting to note that early in the displacement record, the dummy's velocity corresponded closely with that predicted for a man standing broadside to the wind ( $\alpha = 0.052 \text{ ft}^2/\text{lb}$ ; see Table 5.1). At later times, because of rotation, the dummy's increase in velocity with time corresponded more closely with that predicted for a prone man aligned with the wind (see lower curve on Fig. 5.1). It should be noted that the record obtained for the dummy was terminated because dust obscured the test area; therefore, the latter part of the record was less accurately determined than the initial portion. There was some indication that the dummy's velocity was increasing slightly at the termination of the record. However, if 21.4 ft/sec is assumed to have been the maximum velocity attained, then it is possible to determine an acceleration coefficient that would produce a predicted maximum velocity of the same value (21.4 ft/sec) under the same blast conditions. The effective acceleration coefficient so determined had a value of  $0.0268 \text{ ft}^2/\text{lb}$ . This is remarkably close to  $0.03 \text{ ft}^2/\text{lb}$  computed

TABLE 5.1—TYPICAL ACCELERATION COEFFICIENTS ( $\alpha$ )

	$\alpha$ , ft <sup>2</sup> /lb	Reference
168-lb man:		
Standing facing wind	0.052	1
Standing sidewise to wind	0.022	1
Crouching facing wind	0.021	1
Crouching sidewise to wind	0.017	1
Prone aligned with wind	0.0063	1
Prone perpendicular to wind	0.022	1
Average value for tumbling man in straight, rigid position	0.030	2
21-g mice, maximum presented area	0.38	2
180-g rats, maximum presented area	0.19	2
530-g guinea pigs, maximum presented area	0.15	2
2100-g rabbits, maximum presented area	0.079	2
Typical stones:		
0.1 g	0.67	2
1.0 g	0.32	2
10.0 g	0.15	2
Window-glass fragments, $\frac{1}{8}$ in. thick:		
0.1 g, all orientations	0.78	2
1.0 g, edgewise and broadside to wind	0.48–0.57	2
10.0 g, edgewise and broadside to wind	0.34–0.72	2
Steel spheres:		
$\frac{1}{8}$ in. diameter	0.139	3
$\frac{1}{4}$ in. diameter	0.0696	3
$\frac{7}{16}$ in. diameter	0.0398	3
$\frac{1}{2}$ in. diameter	0.0348	3
$\frac{9}{16}$ in. diameter	0.0310	3

for a tumbling man in a straight, rigid position (see Table 5.1). Using the latter value, a predicted maximum velocity of 23.4 ft/sec was obtained in a displacement of 19.5 ft (see plotted point in Figure 5.1). The total displacement of the dummy, measured after the event, was 21.9 ft. This figure included, of course, the distance required for the dummy to come to a stop after maximum velocity had been reached, and therefore it cannot be compared directly with displacement predicted at the time of maximum velocity.

Other field studies<sup>5,6</sup> have been made to evaluate the velocities of glass-fragment missiles originating from windows facing the oncoming blast wave (the window frames were mounted in the open and in houses). It was found in the case of the house-mounted windows that a considerable portion of the missile sample from each window had velocities higher than could be explained if acceleration coefficients noted in Table 5.1 were used in applying the results of the present study to the blast situations encountered in the field operations. However, if one computed on the basis of a reflected blast wave, the higher missile velocities were satisfactorily explained. Thus, it appears that the somewhat complicated hydrodynamic phenomena occurring when a blast wave enters a house by way of a window or windows produces missile results equivalent to a shock overpressure more than twice as great as the overpressure actually incident upon the house.

Acceleration coefficients for steel spheres have been included in Table 5.1 for comparative purposes. For instance, the alphas for a tumbling man and a steel sphere  $\frac{9}{16}$  in. in diameter are about the same. Similarly,  $\frac{1}{8}$  in. steel spheres and guinea pigs are approximately equivalent in so far as translation by blast waves is concerned. Thus, in theory, an "equivalent" sphere can be found for any irregular object. This concept has been used in weapon-effects tests<sup>4,6</sup> taking advantage of the fact that velocity can be experimentally determined more readily for a sphere than for the object it represents.

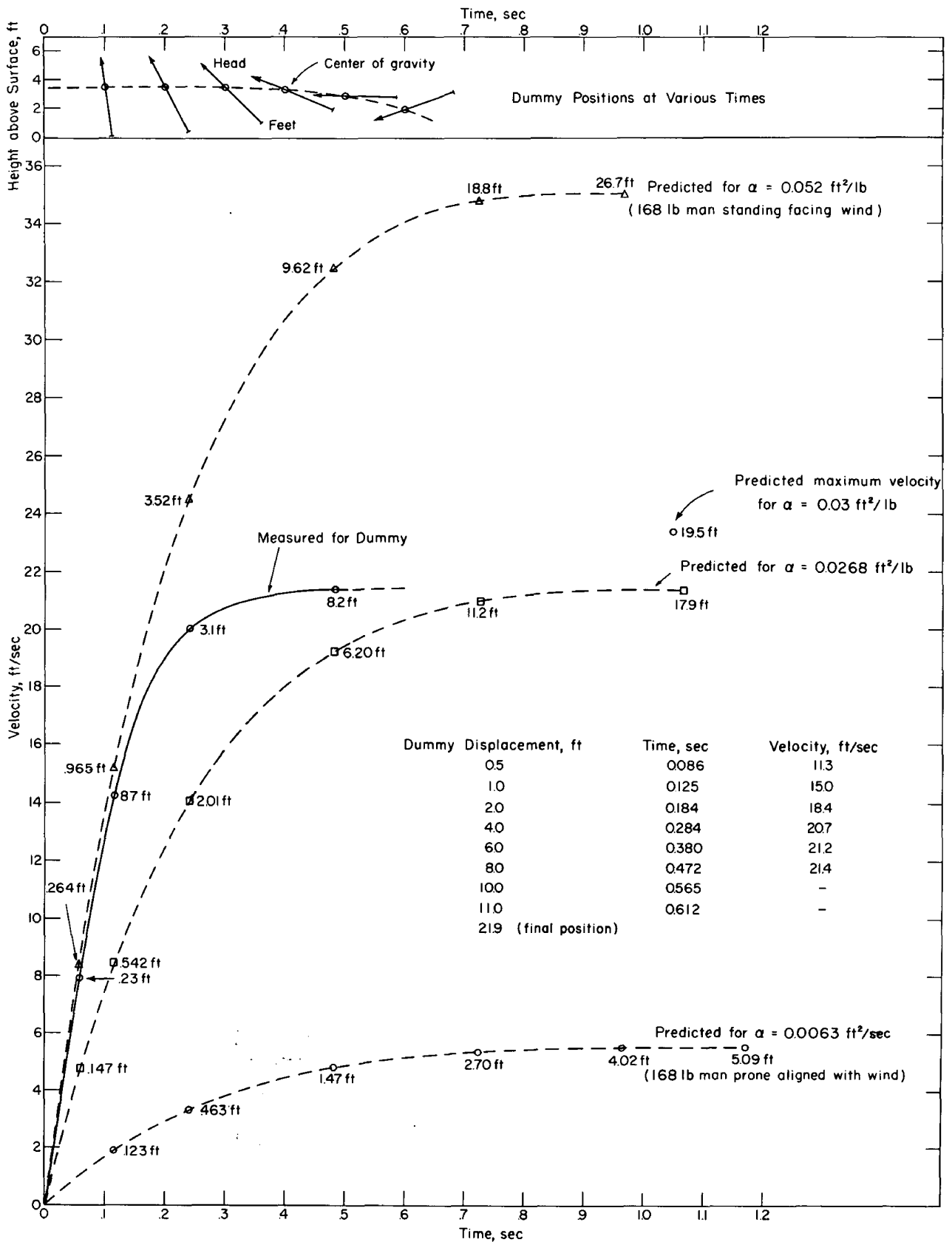


Fig. 5.1—Anthropometric dummy translation history, obtained from full-scale weapon test,<sup>4</sup> compared with that predicted using various values of acceleration coefficient (see Table 5.1) and the computed data in Table 4.1. Numbers adjacent to plotted points indicate measured or computed displacements. Blast parameters:  $p_s = 5.3 \text{ psi}$ ,  $p_0 = 13.3 \text{ psi}$ ,  $t_p^+ = 0.964 \text{ sec}$ ,  $c_0 = 1120 \text{ ft/sec}$ .

### 5.3 WEAPON YIELD AS A BLAST PARAMETER

Although the motion parameters were evaluated without regard to yield, introduction of the latter at this point is both interesting and useful. Employing the well-known weapon-scaling law<sup>7,8</sup> applying to given values of shock overpressures, the following relation can be written:

$$\frac{t_p^+}{(t_p^+)_1} = \frac{t_u^+}{(t_u^+)_1} = \left[ \frac{W(p_0)_1}{W_1 p_0} \right]^{1/3} \frac{(c_0)_1}{c_0} \quad (5.1)$$

Quantities marked with the subscript "1" are considered to be constant and to have reference or "standard" values. The parameters not so marked can take any set of appropriate values.

The next step is taken from the definitions of dimensionless acceleration coefficient (A) and displacement (D). The subscript marking is similar to that for Eq. 5.1.

$$\left( \frac{\alpha p_0 t_u^+}{c_0} \right)_1 = \frac{\alpha p_0 t_u^+}{c_0} \quad (5.2)$$

$$\frac{d}{t_u^+ c_0} = \left( \frac{d}{t_u^+ c_0} \right)_1 \quad (5.3)$$

Eliminating  $t_u^+/(t_u^+)_1$  between Eq. 5.1 and Eqs. 5.2 and 5.3, in turn, the following is obtained:

$$\alpha_1 = \alpha \left[ \frac{(c_0)_1}{c_0} \right]^2 \left[ \frac{p_0}{(p_0)_1} \right]^{2/3} \left( \frac{W}{W_1} \right)^{1/3} \quad (5.4)$$

$$d = d_1 \left[ \frac{W}{W_1} \frac{(p_0)_1}{p_0} \right]^{1/3} \quad (5.5)$$

Thus, weapon yield replaces duration as parameter. The significance of this transformation will be demonstrated in Sec. 5.4.

### 5.4 MAXIMUM VELOCITY AND CORRESPONDING DISPLACEMENT

Data in Table 4.1, along with Eq. 2.24, were used to prepare Fig. 5.2, which shows the maximum missile velocity as a function of acceleration coefficient and shock overpressure. The tabulated data were made dimensional for a 1-kt burst where the ambient pressure and speed of sound were 14.7 psi and 1117 ft/sec, respectively. By use of the transformation equation, Eq. 5.4, and the definition of dimensionless velocity, the data on this chart can be made to apply to other conditions where  $W$ ,  $p_0$ , and  $c_0$  may be different from those used in the construction of the chart.

Consider the translation of a man whose average alpha is 0.03 ft<sup>2</sup>/lb. For a 1-kt burst at a range where the shock overpressure is 1 atm, his maximum velocity is predicted to be 37 ft/sec (see Fig. 5.2). If the yield were 1000 kt, however, the adjusted alpha,  $\alpha_1$ , becomes 0.3. Entering this value for alpha on the same chart, again at the 1-atm curve, a maximum velocity of 195 ft/sec is obtained.

Figure 5.3 shows, for a 1-kt burst, displacement at maximum velocity as a function of alpha and shock overpressure, prepared for the same ambient conditions used for Fig. 5.2. Continuing the example used above, the man would be displaced 9 ft when maximum velocity was reached if the yield were 1 kt. However, if it were 1000 kt, his displacement would be  $28 \times 1000^{1/3} = 280$  ft (see Eqs. 5.4 and 5.5).

Figures 5.4 to 5.7 are similar to those described above except that the yields are 20 kt and 1000 kt (1 Mt). The charts prepared for 1 kt could be used for all yields, except for limitations in the range of the abscissa.

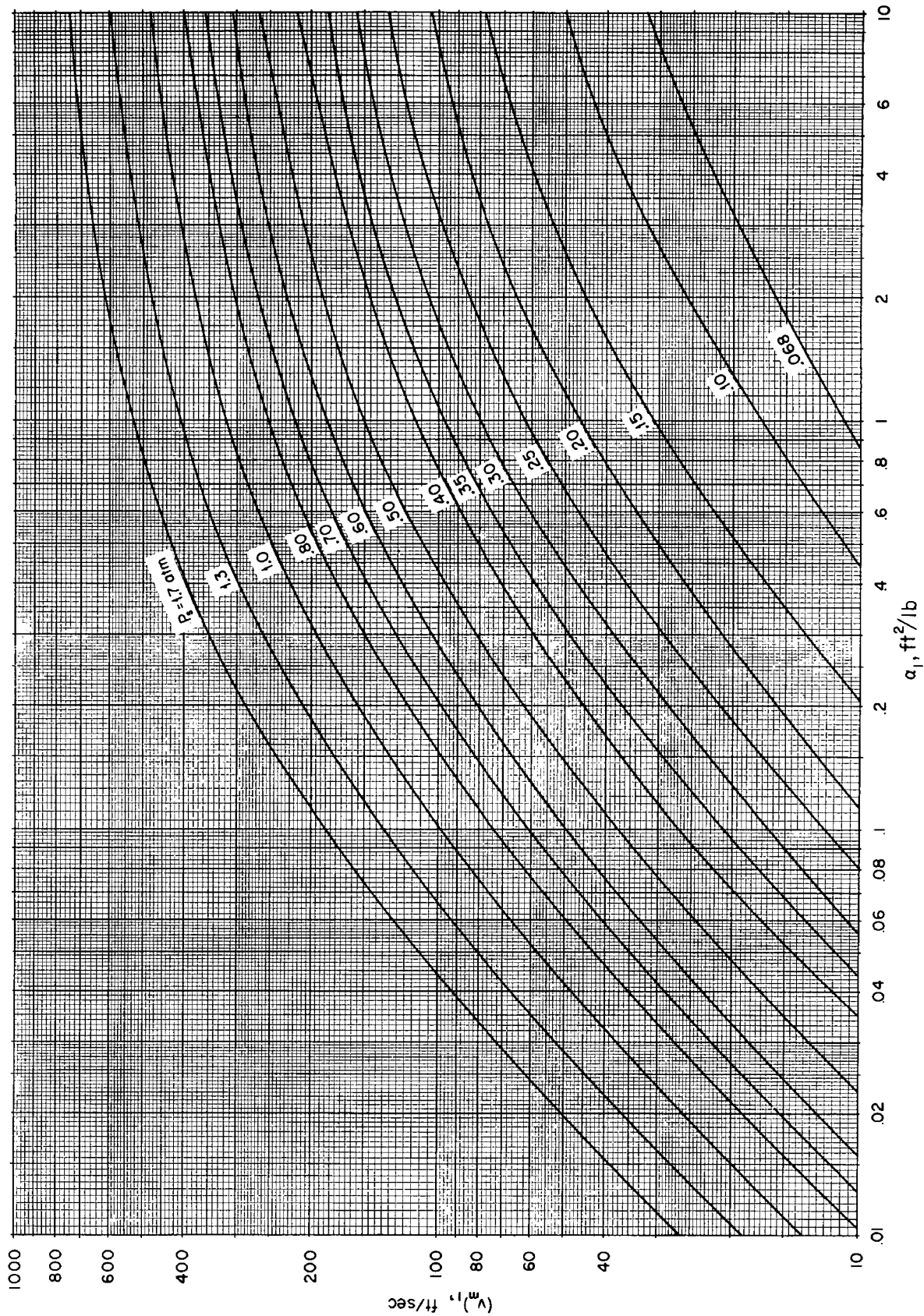


Fig. 5.2—Predicted maximum velocity as a function of acceleration coefficient ( $\alpha$ ) and shock overpressure computed for  $W = 1$  kt,  $P_0 = 14.7$  psi, and  $c_0 = 1117$  ft/sec. For other conditions, use:

$$\alpha_1 = \alpha \left( \frac{1117}{c_0} \right)^2 \left( \frac{P_0}{14.7} \right)^{2/3} W^{1/3}$$

$$v_m = (v_{m\lambda}) \left( \frac{c_0}{1117} \right)$$

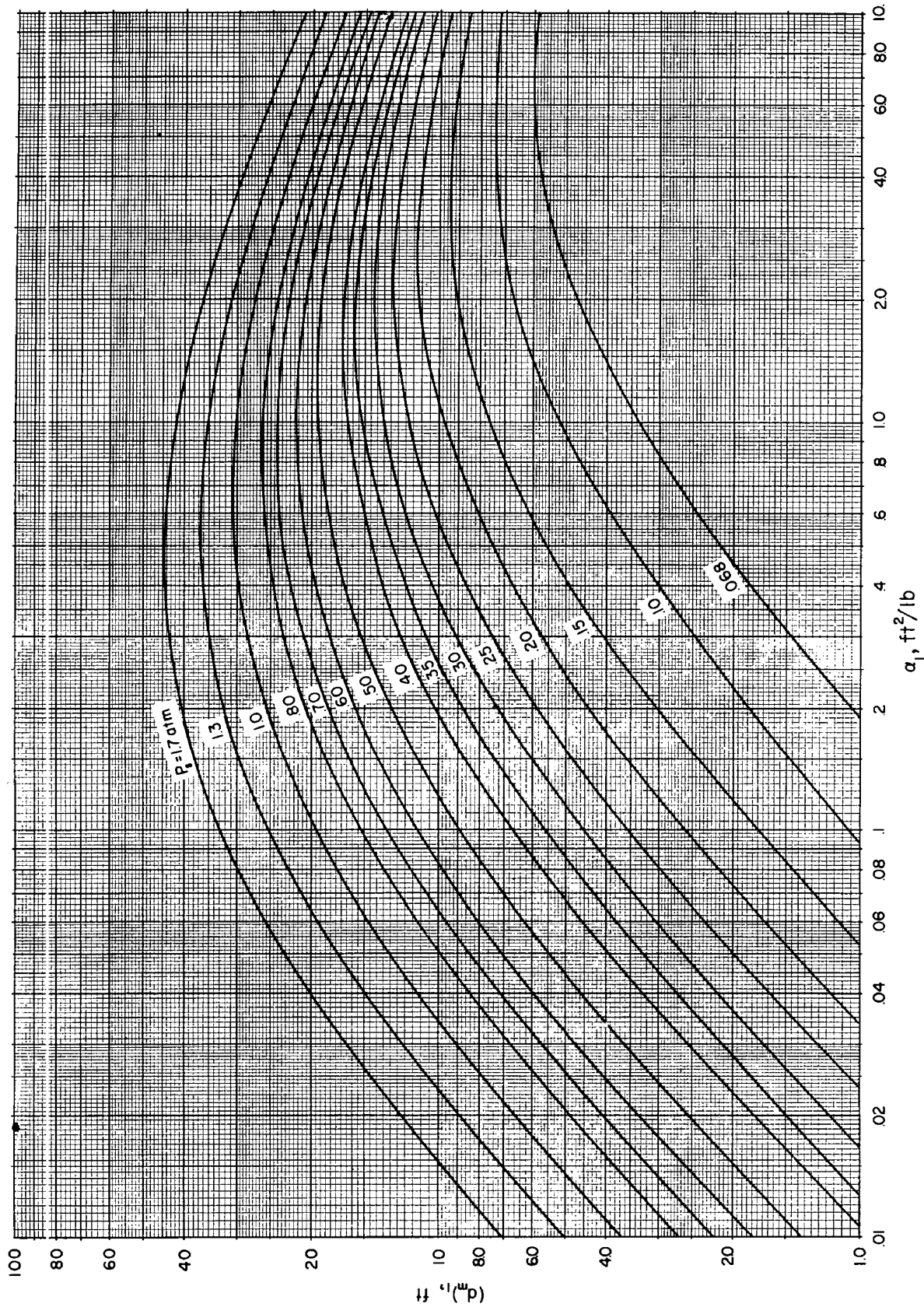


Fig. 5.3—Predicted displacement at maximum velocity as a function of acceleration coefficient ( $\alpha$ ) and shock overpressure computed for  $W = 1$  kt,  $P_0 = 14.7$  psi, and  $c_0 = 111.7$  ft/sec. For other conditions, use:

$$\alpha_1 = \alpha \left( \frac{111.7}{c_0} \right)^2 \left( \frac{P_0}{14.7} \right)^{3/2} W^{1/2} \quad d_m = (d_m)_\lambda \left( \frac{14.7 W}{P_0} \right)^{1/2}$$

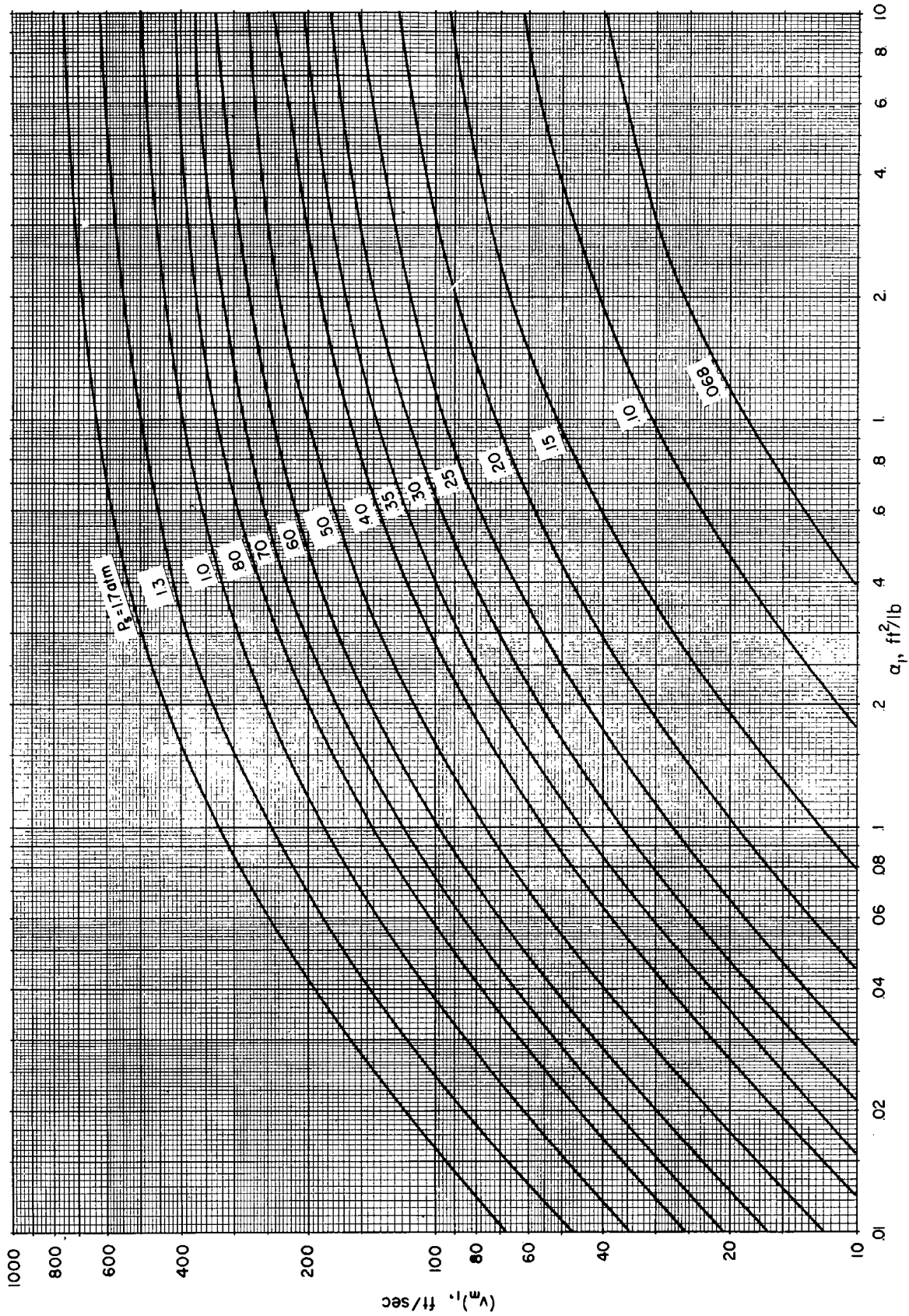


Fig. 5.4—Predicted maximum velocity as a function of acceleration coefficient ( $\alpha$ ) and shock overpressure computed for  $W = 20$  kt,  $P_0 = 14.7$  psi, and  $C_0 = 1117$  ft/sec. For other conditions, use:

$$\alpha_1 = \alpha \left( \frac{1117}{C_0} \right)^2 \left( \frac{P_0}{14.7} \right)^{\frac{2}{3}} \left( \frac{W}{20} \right)^{\frac{1}{2}}$$

$$v_m = (v_m)_0 \frac{C_0}{1117}$$

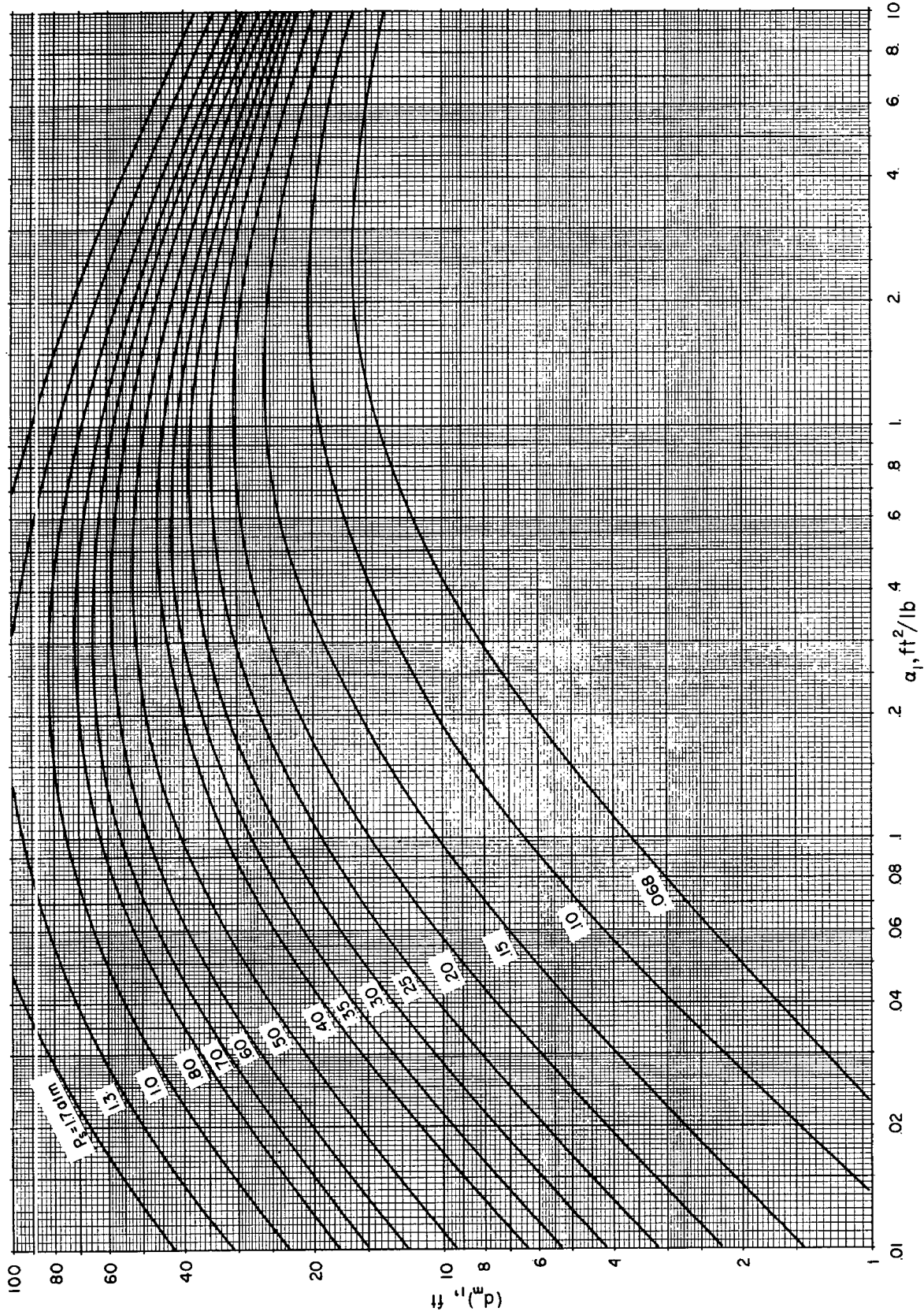


Fig. 5.5—Predicted displacement at maximum velocity as a function of acceleration coefficient ( $\alpha_1$ ) and shock overpressure computed for  $W = 20$  kt,  $p_0 = 14.7$  psi, and  $c_0 = 1117$  ft/sec. For other conditions, use:

$$\alpha_1 = \alpha \left( \frac{1117}{c_0} \right)^2 \left( \frac{p_0}{14.7} \right)^{\frac{1}{2}} \left( \frac{W}{20} \right)^{\frac{1}{2}}$$

$$d_m = (d_m)_\lambda \left( \frac{14.7 W}{p_0} \right)^{\frac{1}{2}}$$



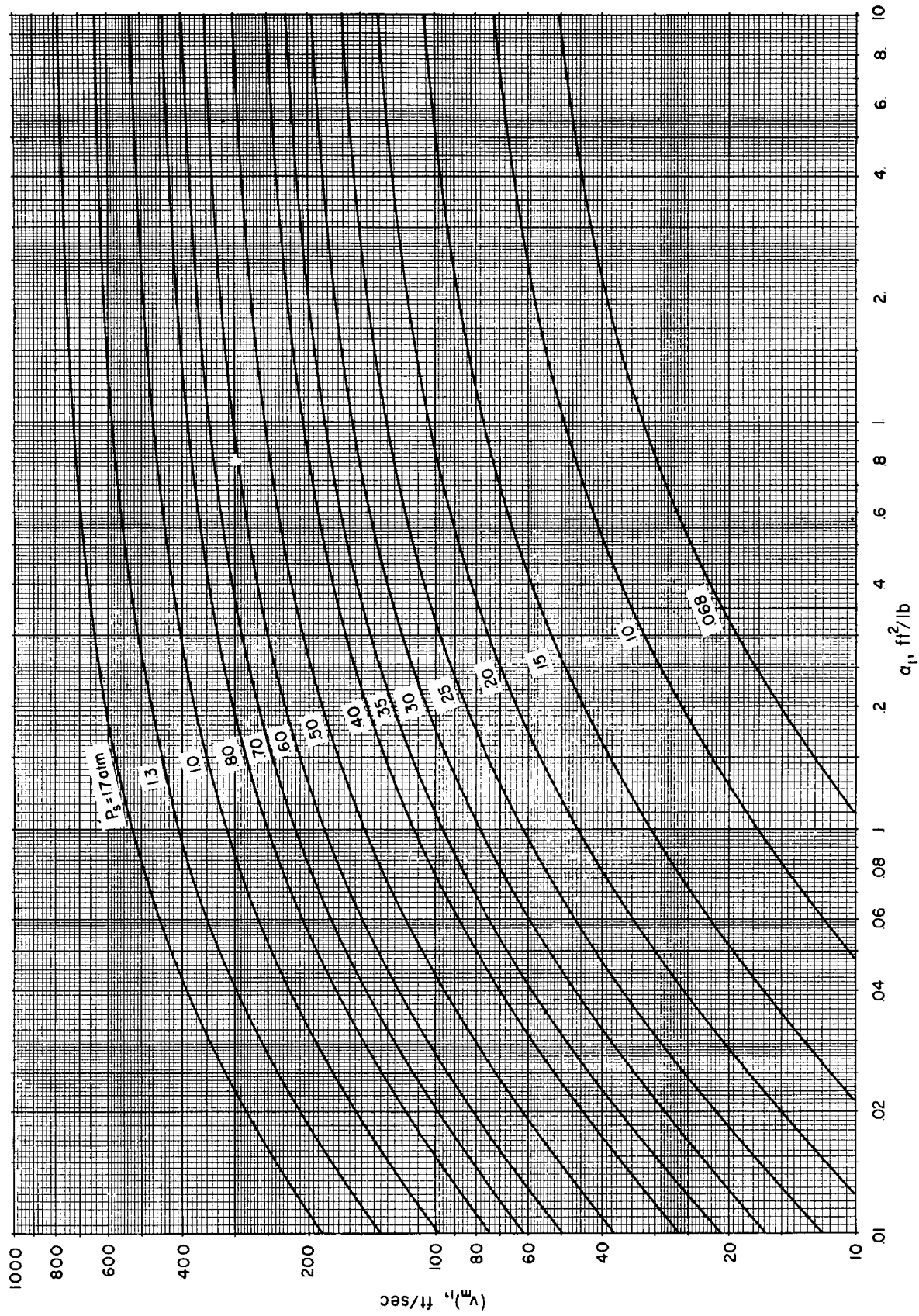


Fig. 5.6—Predicted maximum velocity as a function of acceleration coefficient ( $\alpha$ ) and shock overpressure computed for  $W = 1000$  kt (1 Mt),  $P_0 = 14.7$  psi, and  $c_0 = 1117$  ft/sec. For other conditions, use:

$$\alpha_1 = \alpha \left( \frac{1117}{c_0} \right)^2 \left( \frac{P_0}{14.7} \right)^{3/2} \left( \frac{W}{1000} \right)^{1/2}$$

$$v_m = (v_m)_0 \frac{c_0}{1117}$$

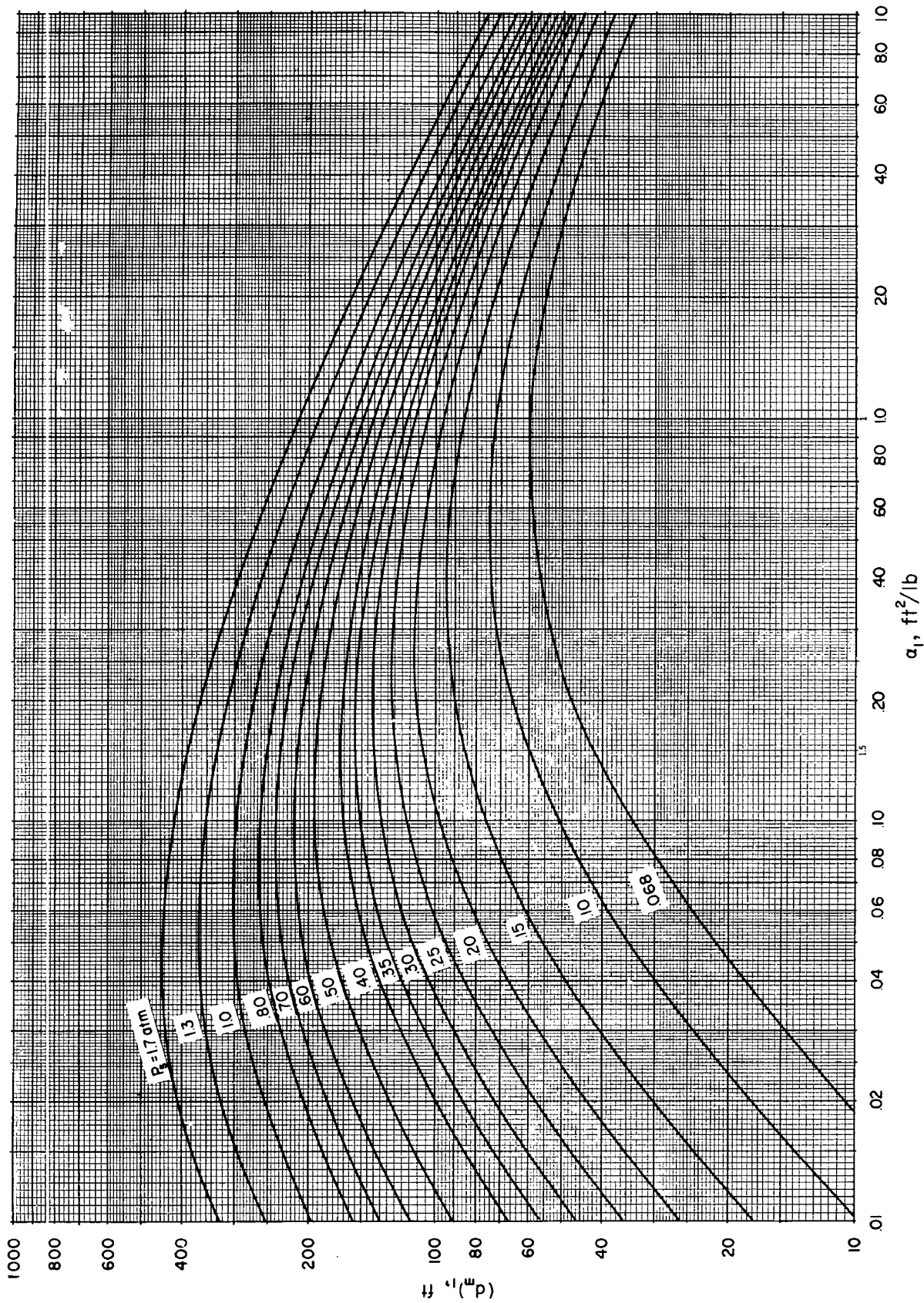


Fig. 5.7—Predicted displacement at maximum velocity as a function of acceleration coefficient ( $\alpha$ ) and shock overpressure computed for  $W = 1000$  kt (1 Mt),  $p_0 = 14.7$  psi, and  $c_0 = 1117$  ft/sec. For other conditions, use:

$$d_m = (d_m) \left( \frac{14.7 W}{p_0 1000} \right)^{1/2} \quad \alpha_1 = \alpha \left( \frac{1117^2}{c_0} \right)^{1/2} \left( \frac{p_0}{14.7} \right)^{1/2} \left( \frac{W}{1000} \right)^{1/2}$$

## 5.5 ESTIMATION OF MAXIMUM VELOCITY FROM TOTAL DISPLACEMENT

Estimation of maximum velocity from total displacement can perhaps be described best by illustration. Suppose an object of unknown  $\alpha$  were exposed to blast winds from a 1-Mt explosion at a location where the ambient pressure and speed of sound were 14.7 psi and 1117 ft/sec, respectively, and the shock overpressure was 0.35 atm (5.14 psi). After the explosion assume a total displacement of 100 ft was measured. This measurement includes, of course, the distance traveled by the object in stopping after maximum velocity had been reached. By use of the plotted data shown in Fig. 5.7, we can only say that the effective  $\alpha$  must have been less than 0.0265. Then, referring to Fig. 5.6, it is determined that for an  $\alpha$  less than 0.0265 under these blast conditions, the maximum velocity must have been less than 45 ft/sec.

The largest source of error in the above estimation, no doubt, embodies the use of total displacement as the displacement at the time of maximum velocity, i.e., "overshoot" was neglected. By means of simple experiments, the amount of overshoot, or stopping distance, could be determined as a function of initial velocity. Inclusion of this factor in the estimation procedure would result in a smaller but more accurate value for estimated maximum velocity.

Assuming that the overshoot is known, what are the assumptions involved in estimating maximum velocity from displacement? Essentially, it is assumed that the velocity-time history of an object is determined by the fact that it traveled a known distance in a known time. Mathematically, any number of velocity-time curves could satisfy the known distance-time values; however, the most likely one is assumed, in the above procedure, to be of the form of computed secondary-missile velocity vs. time for a classical blast wave. It is interesting to note that no previous knowledge of  $\alpha$  is necessary and that an "effective" value is automatically obtained by the analytical procedure. Effective  $\alpha$  could be modified in the real blast situation by such extraneous influences as ground friction or shielding without seriously affecting the accuracy of maximum velocity determined by displacement. However, if the missile were in the air at a considerable height at the time of maximum velocity and if the latter were fairly high, the estimate of overshoot could be seriously affected.

## 5.6 COMPUTED VELOCITY AND DISPLACEMENT FOR PARTICULAR OBJECTS

### 5.6.1 Interpolation of Alpha and Overpressure

Application of the computed motion parameters to specific objects and blast situations makes it necessary to interpolate between the values of  $\alpha$  and/or shock overpressure for which computations were made. It has been found that linear interpolation produces results sufficiently accurate for most purposes. Graphic interpolation has also been found to produce satisfactory results. Charts prepared by such procedures will be presented later in this section.

### 5.6.2 Velocity and Displacement Predicted for Man and for Glass Fragments

Figure 5.8 was prepared, primarily, to illustrate the effect of yield on the velocity and displacement predicted for a tumbling man and 10-g fragments of glass arising from a window in a house (see Table 5.1  $\alpha$  values). The predictions apply to a shock overpressure of 5.14 psi, ambient pressure of 14.7 psi ( $P = 0.35$  atm), and speed of sound of 1117 ft/sec. Also shown on Fig. 5.8 are the ranges from Ground Zero as a function of weapon yield where the stated shock overpressure could be expected to occur for a surface burst and a "typical" air burst.<sup>7</sup>

For illustrative purposes, the steps taken in the preparation of Fig. 5.8 are outlined. Velocity-displacement relations were sought for six yields from 1 kt to 20 Mt. For each yield, wind durations were computed for  $P = 0.35$ ,  $p_0 = 14.7$  psi, and  $c_0 = 1117$  ft/sec, using Eq. 2.24 and Fig. 2.2. Dimensionless  $\alpha$ ,  $A$ , was then computed for each of the yield values used. The next step was to obtain velocity-displacement data from Table 4.1 for  $P = 0.35$ . For each of the times ( $T$ ) listed in this table, corresponding values of velocity and displacement were computed by linear interpolation for the exact value of dimensionless  $\alpha$  applicable to the yield being processed. Then velocity was plotted as a function of displacement for each of the

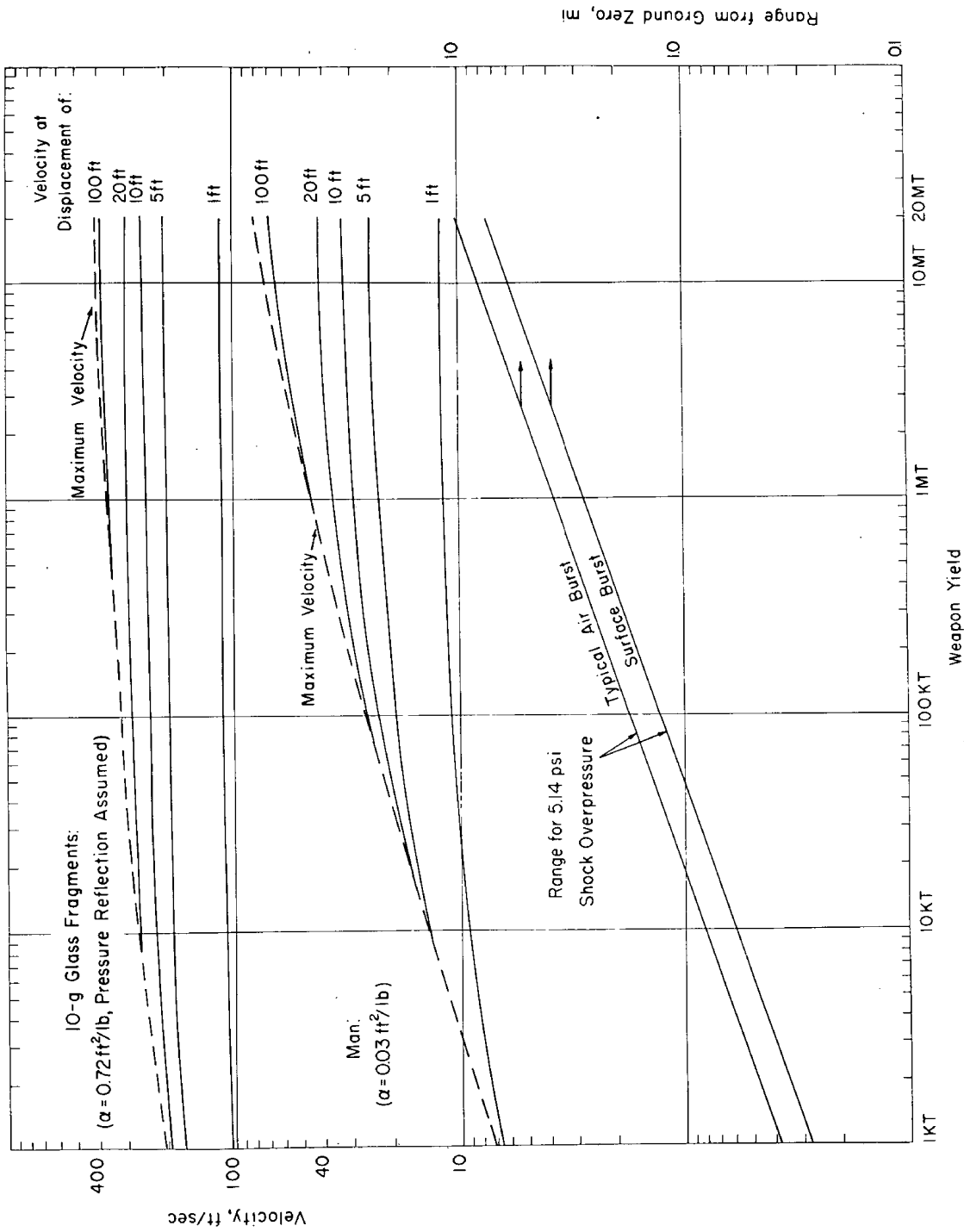


Fig. 5.8—Relation between velocity and displacement as a function of weapon yield computed for 10-g glass fragments and man, where  $p_s = 5.14$ ,  $p_0 = 14.7$  psi, and  $c_0 = 1117$  ft/sec. Range from Ground Zero where predicted data apply is shown as a function of weapon yield.

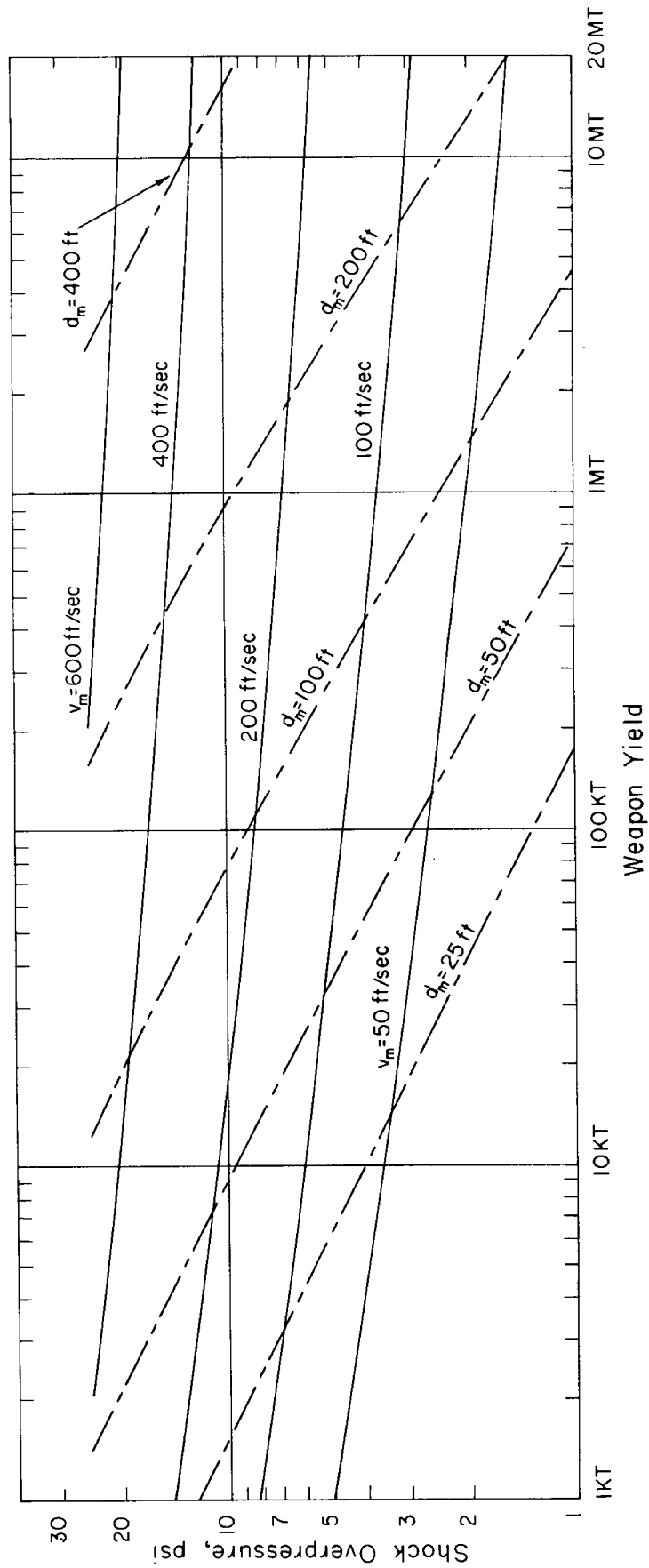


Fig. 5.9—Relation between shock overpressure and yield for various values of maximum velocity and displacement at maximum velocity computed for 1-g stones, where  $\alpha = 0.32 \text{ ft}^2/\text{lb}$ ,  $p_0 = 14.7 \text{ psi}$ ,  $c_0 = 1117 \text{ ft/sec}$ ,  $v_m =$  computed maximum velocity, and  $d_m =$  displacement at maximum velocity.

six yields. Velocities were obtained from these plots at given displacement intervals until maximum velocity was reached. These data, along with the computed maximum velocities, were then used to plot the curves appearing in Fig. 5.8.

The procedure described above applies strictly to the treatment of the data for man. For the 10-g window-glass fragment study, it was assumed that the incident shock overpressure of 0.35 atm was reflected to 0.80 atm (see Sec. 5.2).

The plotted data appearing in Fig. 5.8 indicate that the velocity predicted for man is much more yield dependent than that for glass fragments. The reason for this is that the window glass having a higher alpha reaches wind velocity in a shorter time than does the man and therefore utilizes less of the longer duration produced by higher yield.

It is interesting to note that, for all yields, in only 1 ft of travel the glass fragments have already attained velocities greater than 100 ft/sec. Similarly, for all yields greater than 20 kt, man is predicted to be propelled at more than 10 ft/sec in just 1 ft of travel.

### 5.6.3 Predicted Maximum Velocities and Corresponding Displacements for 1-g Stones

The purpose of this analysis was to study the interplay of the effects of shock overpressure and weapon yield on the velocity and displacement of 1-g stones. The results, shown in Fig. 5.9, were plotted so that corresponding values of shock overpressure and weapon yield could be obtained for the plotted values of maximum velocity and displacement at maximum velocity. Data for this chart were scaled from those presented in Figs. 5.2 and 5.3.

An interesting concept to be derived from this analysis is that of "equivalent" shock overpressures; e.g., a 15-psi blast wave produced by a 1-kt burst is equivalent to a 5.7-psi wave from a 20-Mt burst in that both are predicted to propel 1-g stones at maximum velocities of 200 ft/sec. It should be pointed out, however, that the distances required to achieve maximum velocity are quite different. For the 1-kt burst the required distance is about 30 ft; whereas, for the 20-Mt burst it is about 300 ft.

From the data plotted in Fig. 5.9, it can be concluded that both velocity and displacement increase with pressure and yield; however, missile velocity is more sensitive to pressure (wind-velocity dependence) than is displacement; and, conversely, displacement is more sensitive to yield (duration effect) than is velocity.

## REFERENCES

1. Thomas J. Schmitt, Wind-Tunnel Investigation of Air Loads on Human Beings, Report 892 (Aero 858), The David W. Taylor Model Basin Aerodynamics Laboratory, Washington, D. C., January 1954.
2. E. Royce Fletcher et al., Determination of Aerodynamic Drag Parameters of Small Irregular Objects by Means of Drop Tests, Civil Effects Test Operations, Report CEX-59.14 (in preparation).
3. Sighard F. Hoerner, author and publisher, *Fluid-Dynamic Drag*, Chap. III, pp. 3-8, Midland Park, N. J., 1958.
4. R. V. Taborelli, I. G. Bowen, and E. R. Fletcher, Tertiary Effects of Blast-Displacement, Operation Plumbbob Report, WT-1469, May 22, 1959.
5. I. G. Bowen, A. F. Strehler, and Mead B. Wetherbe, Distribution and Density of Missiles from Nuclear Explosions, Operation Teapot Report, WT-1168, March 1956.
6. I. G. Bowen et al., Secondary Missiles Generated by Nuclear-produced Blast Waves, Operation Plumbbob Report, WT-1468 (in preparation).
7. Samuel Glasstone (Ed.), *The Effects of Nuclear Weapons*, Superintendent of Documents, U. S. Government Printing Office, Washington, D. C., June 1957.
8. Harold L. Brode, Point Source Explosion in Air, Report AECU-3517, The Rand Corporation, Dec. 3, 1956.

## Chapter 6

### DISCUSSION

Although this study was intended to further the understanding of the secondary and tertiary effects of blast on a biological subject, the results are equally applicable to certain other investigative efforts, e.g., studies of physical damage resulting from secondary missiles or displacement. The model that was constructed to describe the motion of objects displaced by the blast wave requires no knowledge of the object displaced except its area presented to the wind, mass, and drag coefficient, all of which are assumed to be constant throughout the duration of the blast wave. In addition, the model requires that other forces which may be present, such as gravity and friction due to the object's moving over a surface, be negligible in comparison with those due to blast winds.

Thus, like most models, certain simplifying assumptions were made (see Sec. 1.3) in the interest of feasibility, simplicity, and uniformity. The determination of whether or not the results so computed apply with sufficient accuracy to particular situations is the subject of other investigations; in particular, those conducted in connection with full-scale nuclear weapons tests, the results of which<sup>1</sup> will be published soon. These field studies included the measurement of velocities for stones and spheres placed in open areas and also for fragments of glass from windows mounted in houses and in open areas. Experiments were conducted in locations where the incident blast wave varied from classical to nonclassical types. One experiment was conducted inside a shelter with an open entryway making use of steel spheres to estimate the velocities at which man might be translated. Other observations made under full-scale test conditions used dogs to assess the hazards of secondary missiles in houses and in open areas<sup>2</sup> and to evaluate the effects of overpressure and displacement inside protective shelters with open entryways.<sup>3,4</sup>

The model dealt with in the present study describes the motion of a missile up to the time of maximum velocity, i.e., when the missile velocity is the same as that of the wind. For some applications a more sophisticated model might be desired which would take into account surface-friction forces during both accelerative and decelerative phases of displacement as well as the decelerative wind forces that occur after maximum velocity has been reached. Such a model would have application to large objects in situations where lofting is not likely to occur. Since total displacement, not displacement at maximum velocity, might be predicted, a model could be used to interpret field data where only total displacement was measured; i.e., total displacement along with appropriate blast data might be sufficient to reconstruct the velocity-time history of the object. It is important to note that this technique need not require a prior knowledge of the object's presented area, mass, or drag coefficient.

Again, it must be pointed out that the missile model described here applies to an ideal or classical blast wave. However, it is well known that blast waves may be modified during their passage through a building or into a structure<sup>3-6</sup> and by the properties of the terrain over which they pass.<sup>1,7,8</sup> Thus, atypical or nonclassical wave forms can and do exist. The important point is that empirical data are at hand for missiles energized by such wave forms. Construction of a theoretical model to predict the behavior of displaced objects under such circumstances can and should be carried out using the experimental data available as a check on the analytical procedures.

Such a model could supplement the present study of blast displacement of objects and allow extension of such thinking to aid in the estimation of missile and displacement damage to man somewhat along the lines of a recent study,<sup>9</sup> which tentatively set forth estimated maximal ranges for human hazards from missiles and displacement wherein the explosive yields were 1 and 10 Mt from an explosive source detonated at the surface of the earth at sea level.

#### REFERENCES

1. I. Gerald Bowen et al., Secondary Missiles Generated by Nuclear-Produced Blast Waves, Operation Plumbbob Report, WT-1468 (in preparation).
2. V. C. Goldizen, D. R. Richmond, and T. L. Chiffelle, Missile Studies with a Biological Target, Operation Plumbbob Report, WT-1470, January 1961.
3. D. R. Richmond et al., Blast Biology—A Study of the Primary and Tertiary Effects of Blast in Open Underground Protective Shelters, Operation Plumbbob Report, WT-1467, June 30, 1959.
4. C. S. White et al., The Biological Effects of Pressure Phenomena Occurring Inside Protective Shelters Following a Nuclear Detonation, Operation Teapot Report, WT-1179, October 1956.
5. B. B. Dunne and Benedict Cassen, Behavior of Shock Waves Entering Model Bomb Shelters, Report UCLA-332, University of California at Los Angeles, April 1955.
6. Russell E. Duff and Robert N. Hollyer, Jr., The Diffraction of Shock Waves Through Obstacles with Various Openings in Their Front and Back Surfaces, Report 50-3, University of Michigan, Nov. 7, 1950.
7. R. Hetherington, Notes on a Steady Solution of the Refraction of a Blast Wave by a Region of Preheated Air, FWE/62, pp. 23-36, Gt. Brit. Armament Research and Development Establishment, July 25, 1958.
8. A. B. Willoughby, K. Kaplan, and N. R. Wallace, Blast Shielding in Complexes, Report AFSWC-TR-57-29, Broadview Research Corporation, August 1958.
9. C. S. White, Biological Blast Effects, presented before the Special Subcommittee on Radiation of the Joint Committee on Atomic Energy During Public Hearings on The Biological and Environmental Effects of Nuclear War, Washington, D. C., June 24, 1959, Report TID-5564.



## Appendix A

### APPROXIMATION METHODS TO SUPPLEMENT THE COMPUTED RESULTS

#### A.1 GENERAL REMARKS

The approximation methods previously described required lengthy computations for numerical solution, although the accuracy attained was satisfactory for a wide range of values of acceleration coefficient. It was realized that other approximation methods could be devised which would require little computational effort but that these methods would be valid only for special conditions, i.e., for short times after the arrival of the blast wave and for very large or for very small acceleration coefficients. Results of these approximations would serve a twofold purpose, that of extending and that of checking the computed results presented in Table 4.1. Material presented in this appendix describes the steps taken to accomplish this purpose.

#### A.2 EQUATIONS OF MOTION APPLYING FOR SHORT TIMES AFTER ARRIVAL OF THE BLAST WAVE

For short periods after the arrival of the blast wave, the acceleration an object experiences may be considered to be constant. Implicit in the above statement is the assumption that the blast wind and dynamic pressure do not decay and that missile velocity is small compared to both the wind and shock velocities. Thus, stated mathematically in numeric form

$$\frac{dV}{dZ} \equiv \dot{V} = Q_s A \quad (\text{A.1})$$

which, upon integration from zero to Z time and from zero to V velocity gives

$$V = Q_s A Z = \frac{dD}{dZ} \quad (\text{A.2})$$

Integrating again between the same time values and between zero and D distance

$$D = Q_s A Z^2 / 2 \quad (\text{A.3})$$

If Eqs. A.2 and A.3 are combined to eliminate Z, the following is obtained

$$V^2 = 2Q_s A D \quad (\text{A.4})$$

$Q_s$  was evaluated for  $P_s = 1.7$  using the equation presented in Sec. 2.3.2, and Eq. A.4 was used to compute V as a function of D for A values of 0.1 and 30. The relations between V and D thus computed are shown graphically in Figure A.1 as dashed straight lines labeled A = 0.1 and A = 30. The curved solid lines that approach tangentially the above mentioned straight lines

were drawn from the computed data presented in Table 4.1. It is interesting to note that at  $T = 0.03$ , the approximation is still fairly good for the case where  $A = 0.1$  in contrast to that for  $A = 30$  at the same time  $T$ .

### A.3 EQUATIONS OF MOTION FOR OBJECTS WITH SMALL ACCELERATION COEFFICIENTS

If an object's acceleration coefficient is sufficiently small, it can be assumed that the velocity attained in a blast situation will be small compared to the wind and shock velocities. Thus, Eq. 2.7 reduces to

$$\frac{dV}{dZ} \equiv \dot{V} = AQ \quad (A.5)$$

Using zero as the initial value of time and velocity, the above expression can be integrated to give

$$V = A \int_0^Z Q dZ = \frac{dD}{dZ} \quad (A.6)$$

Equation A.6 can be integrated similarly to give

$$D = A \int_0^Z \int_0^Z Q dZ dZ \quad (A.7)$$

Combining Eqs. A.6 and A.7 to eliminate  $A$ , the following is obtained

$$\frac{V}{D} = \frac{\int_0^Z Q dZ}{\int_0^Z \int_0^Z Q dZ dZ} \quad (A.8)$$

The evaluation of the above integrals can be accomplished by use of Eq. 2.16

$$\int_0^Z Q dZ = Q_s \left[ \left( \frac{J}{\gamma} e^{-\gamma Z} + \frac{K}{\delta} e^{-\delta Z} \right) (Z - 1) + \frac{J}{\gamma^2} e^{-\gamma Z} + \frac{K}{\delta^2} e^{-\delta Z} + \left( \frac{J}{\gamma} + \frac{K}{\delta} - \frac{J}{\gamma^2} - \frac{K}{\delta^2} \right) \right] \quad (A.9)$$

and

$$\int_0^Z \int_0^Z Q dZ dZ = Q_s \left[ - \left( \frac{J}{\gamma^2} e^{-\gamma Z} + \frac{K}{\delta^2} e^{-\delta Z} \right) (Z - 1) - \left( \frac{2J}{\gamma^3} e^{-\alpha Z} + \frac{2K}{\delta^3} e^{-\delta Z} \right) + \left( \frac{J}{\gamma} + \frac{K}{\delta} - \frac{J}{\gamma^2} - \frac{K}{\delta^2} \right) Z - \left( \frac{J}{\gamma^2} + \frac{K}{\delta^2} - \frac{2J}{\gamma^3} - \frac{2K}{\delta^3} \right) \right] \quad (A.10)$$

The relations derived above were used to describe  $V$  as a function of  $D$  for a 1.7-atm blast wave. These solutions are shown in Fig. A.1 as dashed straight lines for  $T$  values of 0.03,

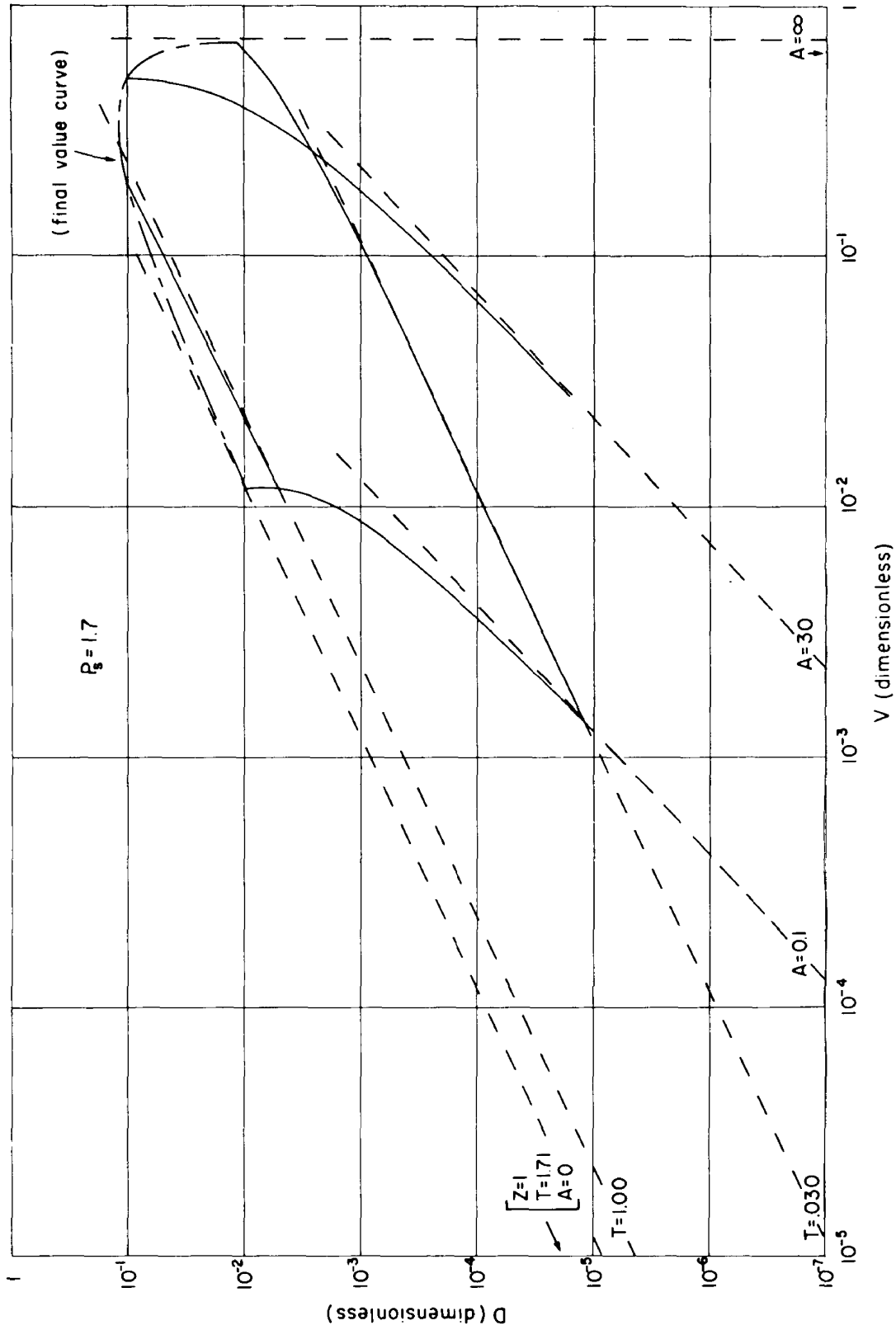


Fig. A.1 — Relation between velocity, displacement, and time after arrival of the blast wave (1.7-atm shock overpressure) computed for several values of acceleration coefficient. The solid curves represent accurately computed data, and the dashed lines represent the data derived from approximation methods developed in the appendix. The solid curves were not extrapolated beyond the data presented in Table 4.1.

1.00, and 1.71. For comparative purposes the accurately computed data from Table 4.1 were used to plot the solid curves, which deviate from the approximation lines at the higher values of V and D. It should be noted that for this blast wave ( $P_s = 1.7$ ),  $T = 1.71$  corresponds to  $Z = 1.0$ , i.e., it is assumed for this approximation that the missile was influenced by the entire positive phase of the blast wave. This, clearly, is the limiting case since it requires that the velocity gained by zero and thus  $A = 0$ . In spite of these assumptions, this approximation (see dashed line for  $Z = 1.0$ , Fig. A.1) is in fair agreement with the "final-value curve" at  $A = 0.1$ .

The relation between  $D_m$  and A is illustrated in Fig. A.2 for three values of  $P_s$ . As in the previous chart, the solid curves were obtained from the accurately computed data and the dashed lines represent approximate relations, which are accurate only for extreme values of A. Equation A.7, with limits on Z from zero to 1, was used to compute the approximation lines for small values of A. The upper approximation lines appearing on this chart are discussed in the next section.

#### A.4 APPROXIMATION RELATIONS FOR LARGE ACCELERATION COEFFICIENTS

It was found by trial that, for missiles with large acceleration coefficients, it was sufficient to consider the maximum missile velocity equal to the peak wind velocity; however, to estimate missile displacement at maximum velocity, it was necessary to compute by approximation methods missile velocity as a function of time and to take into account the decay of the wind with time.

Wind as a function of time can be approximated (for short times) by a straight-line function, thus

$$U(t) = U_s - BZ \quad (\text{A.11})$$

where B represents the initial slope of the wind-time curve, being a parameter dependent only on  $P_s$ .

Using the basic equation, Eq. 2.7, and the approximation written above, the following is obtained

$$dV = Q_s A \left( \frac{U_s - BZ - V}{U_s} \right)^2 \frac{\dot{X}_s}{\dot{X}_s - U_s} dZ \quad (\text{A.12})$$

In the above equation, Q was approximated by  $Q_s$ ; U by  $U_s$ , except when V is subtracted from U; and V by  $U_s$  for the time-expansion term.

To aid in the solution of the above equation, a new variable is defined,  $S = -(U_s - BZ - V)$ , whose derivative is  $dS = dV + B dZ$ . After appropriate substitutions, Eq. A.12 becomes

$$\frac{dS}{dZ} = \frac{AQ}{U_s^2} \frac{\dot{X}_s}{\dot{X}_s - U_s} S^2 + B \quad (\text{A.13})$$

Since it is desired to integrate from  $V = 0$  when  $Z = 0$  to  $V = U$  when  $Z = Z_m$ , the corresponding limits were determined for S as follows (see Eq. A.11):  $S = -U_s$  when  $Z = 0$  and  $S = 0$  when  $Z = Z_m$ . Thus, application of these limits to the integrated form of Eq. A.13 yields

$$Z_m = \frac{U_s}{\sqrt{AQ_s B} \frac{\dot{X}_s}{\dot{X}_s - U_s}} \tan^{-1} \sqrt{\frac{AQ_s}{B} \frac{\dot{X}_s}{\dot{X}_s - U_s}} \quad (\text{A.14})$$

The arc tan factor in the above equation approaches  $\pi/2$  as A becomes large.

The initial slope of the wind-time relation (Eq. 2.17) was found to be

$$B = U_s (\nu + 1) \quad (\text{A.15})$$

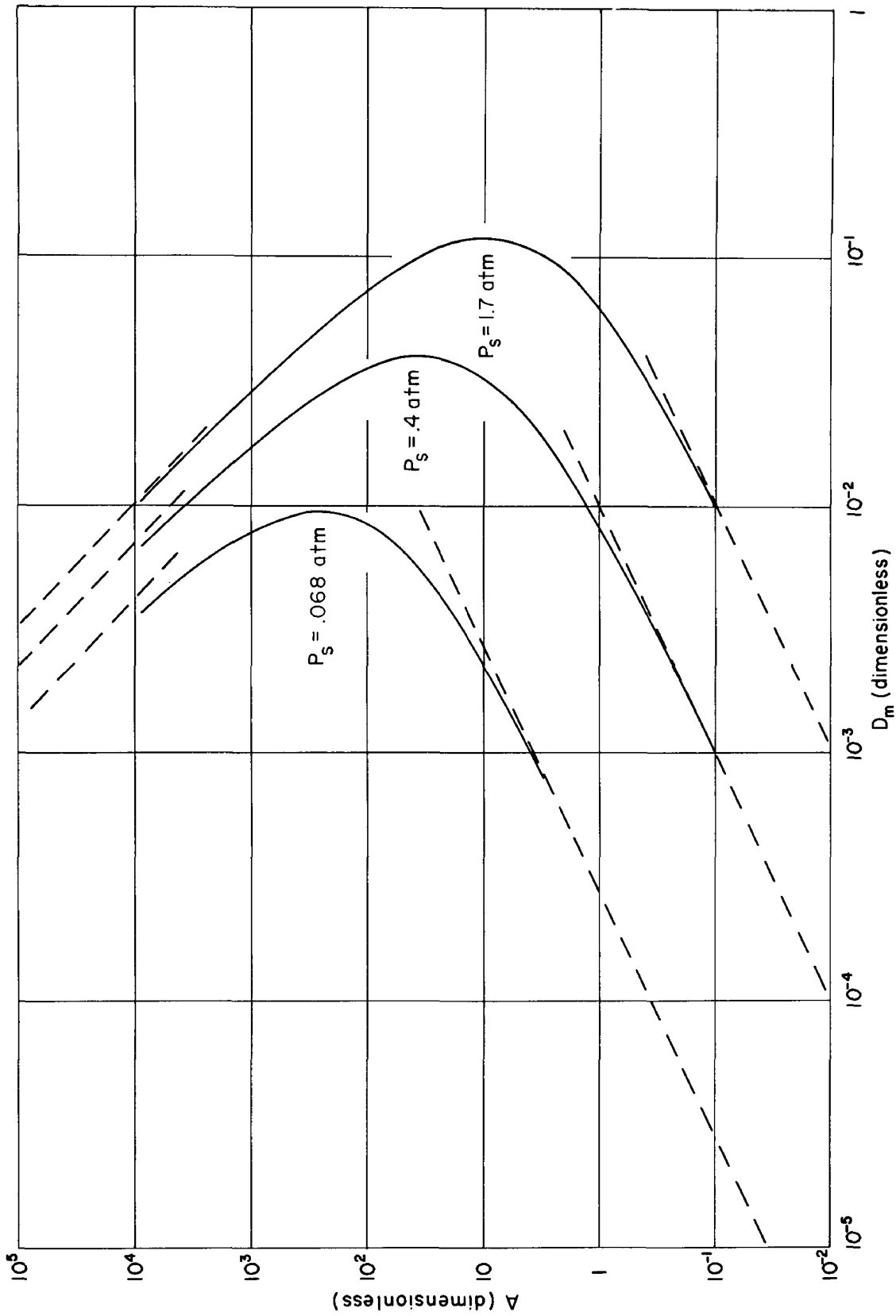


Fig. A.2—Displacement at maximum velocity as a function of acceleration coefficient for various values of shock overpressure. The solid curves represent accurately computed data, and the dashed lines represent the data derived from approximation methods developed in the appendix. The solid curves were not extrapolated beyond the data presented in Table 4.1.

The distance traveled by a missile in reaching maximum velocity is approximately the product of  $V_m$  ( $\approx U_s$ ) and the expanded time (see Sec. 2.2.2) required to reach this velocity.

$$D_m = U_s Z_m \frac{\dot{X}_s}{\dot{X}_s - U_s} \quad (\text{A.16})$$

Substituting Eqs. A.14 (with the evaluation of the arc tan function indicated above) and A.15 into Eq. A.16 yields

$$D_m = \frac{\pi}{2} U_s \sqrt{\frac{U_s}{A Q_s (\nu + 1)} \frac{\dot{X}_s}{\dot{X}_s - U_s}} \quad (\text{A.17})$$

where  $\nu$  is defined as function of  $P_s$  by Eq. 2.17.

Equation A.17 was used to plot the approximation lines for large values of  $A$  appearing in Fig. A.2. It is of interest to note that for a given value of  $A$  ( $10^4$ , for instance) the approximation of  $D_m$  is better for strong blast waves ( $P_s = 1.7$ ) than for weak ones ( $P_s = 0.068$ ). This is probably because in the strong blast wave the missile gains a higher percentage of the peak wind velocity than in the case of the weaker wave.

#### A.5 NORMALIZED VELOCITY VS. DISTANCE FOR MISSILES WITH LOW ACCELERATION COEFFICIENTS

A relation that has proved useful is normalized velocity ( $V/V_m$ ) as a function of normalized distance ( $D/D_m$ ). Computed data from Table 4.1 were used to prepare the plots shown in Fig. A.3 for three values of  $A$  for  $P_s = 0.068$  (1 psi at sea level). These plots illustrate that the smaller the value of  $A$ , the slower is the increase in normalized velocity with increase in normalized distance. Hidden in this relation is the fact that, for a given blast wave, missiles with the smaller values of  $A$  are accelerated over longer times and thus longer distances in relation to their velocities. Nevertheless, it would be interesting to determine if there is a limiting curve of  $V/V_m$  vs.  $D/D_m$  for missiles with  $A$  values approaching zero. To accomplish this, Eqs. A.6 and A.7 were used in the following manner (remembering that the maximum velocity and corresponding displacement are reached at a time,  $Z$ , approaching unity if the value of  $A$  approaches zero):

$$\frac{V}{V_m} = \frac{\int_0^Z Q dZ}{\int_0^1 Q dZ} \quad (\text{A.18a})$$

and

$$\frac{D}{D_m} = \frac{\int_0^Z \int_0^Z Q dZ dZ}{\int_0^1 \int_0^Z Q dZ dZ} \quad (\text{A.18b})$$

The above equations were solved for several corresponding  $Z$  values, and the results were used to plot the curve of  $A = 0$  in Fig. A.3.

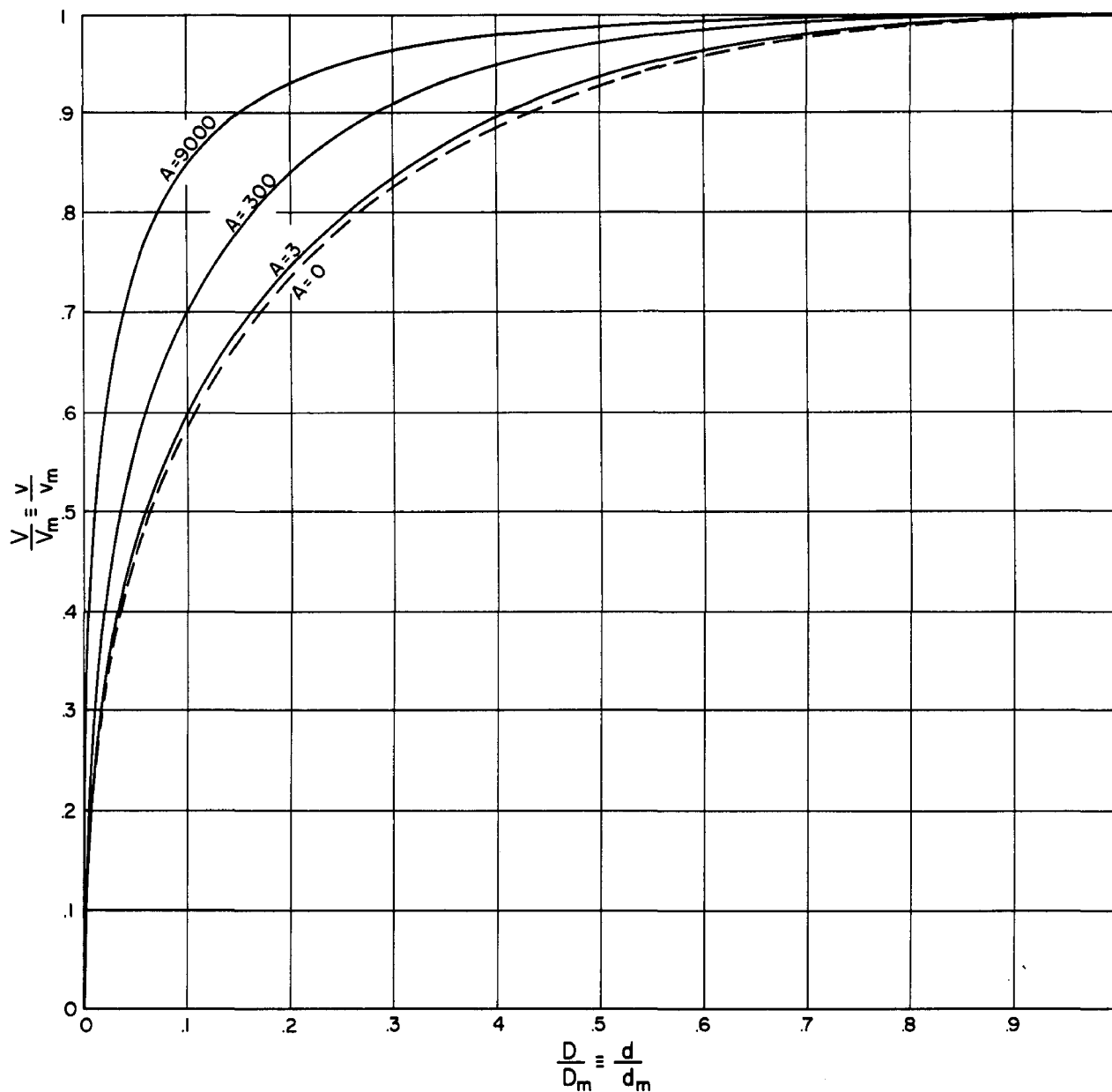


Fig. A.3—Normalized velocity vs. normalized displacement for various values of acceleration coefficient computed for a shock overpressure of 0.068 atm. Data for the solid curves were obtained from Table 4.1, and those for the dashed curve ( $A = 0$ ) were obtained from approximation methods (see Sec. A.5).





## CIVIL EFFECTS TEST OPERATIONS REPORT SERIES (CEX)

Through its Division of Biology and Medicine and Civil Effects Test Operations Office, the Atomic Energy Commission conducts certain technical tests, exercises, surveys, and research directed primarily toward practical applications of nuclear effects information and toward encouraging better technical, professional, and public understanding and utilization of the vast body of facts useful in the design of countermeasures against weapons effects. The activities carried out in these studies do not require nuclear detonations.

A complete listing of all the studies now underway is impossible in the space available here. However, the following is a list of all reports available from studies that have been completed. All reports listed are available from the Office of Technical Services, Department of Commerce, Washington 25, D. C., at the prices indicated.

- CEX-57.1    The Radiological Assessment and Recovery of Contaminated  
(\$0.75)    Areas, Carl F. Miller, September 1960.
- CEX-58.1    Experimental Evaluation of the Radiation Protection Afforded by  
(\$2.75)    Residential Structures Against Distributed Sources, J. A. Auxier,  
J. O. Buchanan, C. Eisenhauer, and H. E. Menker, January 1959.
- CEX-58.2    The Scattering of Thermal Radiation into Open Underground  
(\$0.75)    Shelters, T. P. Davis, N. D. Miller, T. S. Ely, J. A. Basso, and  
H. E. Pearse, October 1959.
- CEX-58.7    AEC Group Shelter, AEC Facilities Division, Holmes & Narver,  
(\$0.50)    Inc., June 1960.
- CEX-58.8    Comparative Nuclear Effects of Biomedical Interest, Clayton S.  
(\$1.00)    White, I. Gerald Bowen, Donald R. Richmond, and Robert L.  
Corsbie, January 1961.
- CEX-59.1    An Experimental Evaluation of the Radiation Protection Afforded  
(\$0.60)    by a Large Modern Concrete Office Building, J. F. Batter, Jr.,  
A. L. Kaplan, and E. T. Clarke, January 1960.
- CEX-59.4    Aerial Radiological Monitoring System. I. Theoretical Analysis,  
(\$1.25)    Design, and Operation of a Revised System, R. F. Merian,  
J. G. Lackey, and J. E. Hand, February 1961.
- CEX-59.13    Experimental Evaluation of the Radiation Protection Afforded by  
(\$0.50)    Typical Oak Ridge Homes Against Distributed Sources, T. D.  
Strickler and J. A. Auxier, April 1960.

